농학박사 학위논문

# 유전체 수준의 벼도열병균 소형 RNA 분석

# Genome-wide analysis of small RNAs in the rice blast fungus, *Magnaporthe oryzae*

2023년 2월

서울대학교 대학원

농생명공학부 식물미생물학전공

이 현 준

# Genome-wide analysis of small RNAs in the rice blast fungus, *Magnaporthe oryzae*

A dissertation submitted in partial
fulfillment of the requirement for
the degree of

**DOCTOR OF PHILOSOPHY**

to the Faculty of
Department of Agricultural Biotechnology

at

**SEOUL NATIONAL UNIVERSITY**

by

**Hyunjun Lee**

FEBRUARY 2023

농학박사 학위논문

# 유전체 수준의 벼도열병균 소형 RNA 분석

지도교수 이 용 환

이 논문을 농학박사 학위논문으로 제출함
2022년 12월

서울대학교 대학원
농생명공학부 식물미생물학전공

이 현 준

이현준의 박사 학위논문을 인준함

2022년 12월

위 원 장 _____ (인)

부 위 원 장 _____ (인)

위 원 _____ (인)

위 원 _____ (인)

위 원 _____ (인)

A THESIS FOR THE DEGREE OF DOCTOR OF PHILOSOPHY

# Genome-wide analysis of small RNAs in the rice blast fungus, *Magnaporthe oryzae*

UNDER THE DIRECTION OF DR. YONG-HWAN LEE

SUBMITTED TO THE FACULTY OF THE GRADUATE SCHOOL OF SEOUL NATIONAL UNIVERSITY

BY

HYUNJUN LEE

PROGRAM IN PLANT MICROBIOLOGY
DEPARTMENT OF AGRICULTURAL BIOTECHNOLOGY

DECEMBER 2022

APPROVED AS A QUALIFIED THESIS OF HYUNJUN LEE
FOR THE DEGREE OF DOCTOR OF PHILOSOPHY
BY THE COMMITTEE MEMBERS

CHAIRMAN _____

VICE CHAIRMAN _____

MEMBER _____

MEMBER _____

MEMBER _____

## ABSTRACT

# Genome-wide analysis of small RNAs in the rice blast fungus, *Magnaporthe oryzae*

Hyunjun Lee
Program in Plant Microbiology
Department of Agricultural Biotechnology
The Graduate School
Seoul National University

RNA interference (RNAi) is a conserved mechanism suppressing gene expression mediated by small RNA (sRNA). sRNA guides RNA-induced silencing complex (RISC) to target mRNA using sequence complementary, regulating genes through mRNA degradation, translational inhibition, or transcriptional repression. Recent studies on the functional characterization of RNAi components exhibited that RNAi plays essential roles in fungal pathogenesis toward host plants. Viral defense and stress tolerance regulated by RNAi are crucial for some plant pathogenic fungi to maintain full virulence. In many plant pathogenic fungi, it has been revealed that fungal sRNAs can be secreted into host plants and modulate host gene expression. These suggest that plant pathogenic fungi exploit RNAi mechanism in diverse processes to orchestrate fungal pathogenesis. Furthermore, non-canonical RNAi

pathways, in which core RNAi components, Dicer or Argonaute, are not involved, were reported to have significant roles in animals, plants, and fungi. However, the relevance of non-canonical RNAi with plant pathogenic fungi has rarely been studied. To comprehensively understand non-canonical, Dicer-independent RNAi in the rice blast fungus, *Magnaporthe oryzae*, Dicer-dependent and -independent sRNAs were profiled. In *M.* oryzae, Dicer-dependent sRNAs were 19-24-nt in length and had low strand-specificity. By contrast, Dicer-independent sRNAs exhibited irregular patterns in length distribution and high strand-specificity. While Dicer-dependent sRNAs showed a preference for uracil at the 5'-end, Dicer-independent sRNAs were biased with cytosine at the penultimate position. Dicer-dependent sRNA loci were mainly associated with LTR-transposons, whereas Dicer-independent sRNAs were associated with protein-coding genes and simple repeats. To decipher the roles of Dicer-independent sRNAs of *M. oryzae*, *MoERI-1*, a homologue of non-canonical RNAi component *ERI*-1 of *Neurospora crassa*, was identified. Δ*Moeri-1* was subjected to sRNA and mRNA sequencing at the mycelia and conidiation stages, as the mutant showed increased conidiation. Deletion of *MoERI-1* upregulated the genes involved in conidiation and cell cycle. Furthermore, a comparison between sRNA and mRNA transcriptome revealed that MoERI-1-dependent sRNAs mediate the regulation of gene expression. Taken together, *M. oryzae* exploits non-canonical RNAi pathway to regulate the conidiation process and the disease development.

**Keywords**: *Magnaporthe oryzae*, sRNA, RNAi, Dicer-independent, MoERI-1

***Student number***: 2014-22938

# CONTENTS

# LIST OF TABLES

## CHAPTER I



## CHAPTER II

# LIST OF FIGURES

**CHAPTER I**

*page*



**CHAPTER II**

*page*

# CHAPTER I

# RNAi in plant pathogenic fungi

This chapter is in preparation for publication.

# ABSTRACT

RNA interference (RNAi) controls cellular processes in eukaryotes using small RNA (sRNA) to suppress gene expression by mRNA degradation, translational inhibition, or transcriptional repression in a sequence-specific manner. In fungi, the functions of RNAi in maintaining genome integrity and adaptation to environments are well known. Recent studies revealed that plant pathogenic fungi exploit RNAi in diverse ways to orchestrate the disease development. RNAi contributes to fungal pathogenesis directly by regulating endogenous virulence genes, or indirectly by controlling the viral RNA or transposon. Moreover, fungal pathogens secrete sRNAs into host plant to modulate the expression of host defense-related genes. It has also been found that non-canonical RNAi mechanisms lacking core RNAi components, such as Dicer or Argonaute, are involved in the fungal pathogenesis toward plant hosts. This review summarizes the functionally characterized RNAi components and sRNAs in plant pathogenic fungi identified to date and discusses their roles in host-pathogen interactions.

# INTRODUCTION

RNA RNA interference (RNAi) is a well-conserved mechanism in which antisense small RNAs (sRNAs) induce the suppression of genes with complementary sequences by mRNA degradation, translation inhibition, and chromatin remodeling. The sRNAs mediating RNAi comprise approximately 18–30 nucleotides. RNAi orchestrates fast and fine-tuned changes in gene expression that are crucial for development, responses to stimuli, and pathogenesis (Kruszka et al. 2012; Biggar and Storey 2015).

Canonical RNAi requires well-conserved core RNAi components Dicer, Argonaute (AGO) and RNA-dependent RNA polymerase (RdRP). Dicer is an RNAse III-like endonuclease that plays an essential role in RNAi; it processes dsRNA and hairpin-structured RNAs into small fragments. These fragments are bound to AGO, which functions as an sRNA-guided endonuclease by identifying target mRNA or DNA loci based on the complementarity of the incorporated sRNA. This cascade of events leads to gene silencing at the transcriptional or post-transcriptional level. RdRPs synthesize and amplify the dsRNA from single-stranded RNAs by primer-independent synthesis of second strands, using sRNAs as primers to produce RNA molecules complementary to the mRNA targets.

Since the first RNA silencing phenomenon, co-suppression of the chalcone synthase gene, was observed in petunia, similar phenomena in fungi and animals revealed that core components of RNAi were highly conserved in eukaryotic

organisms (Fire et al., 1998; Napoli et al., 1990; Romano and Macino, 1992). Quelling, one of the first RNA silencing phenomena, was reported in *Neurospora crassa*, an essential model organism for genetics (Romano and Macino, 1992). As a post-transcriptional gene silencing (PTGS) induced by transgenes homologous to an endogenous gene, quelling suppresses transposons and virus infections (Cogoni and Macino, 1999; Romano and Macino, 1992). In 2000, dsRNAs were confirmed as the triggers of transgene-induced gene silencing, and were converted into the shorter intermediates, small interfering RNAs (siRNAs) (Hammond et al., 2000; Zamore et al., 2000). The first identified sRNA was the lin4 miRNA discovered in *Caenorhabditis elegans* (Lee et al., 1993; Wightman et al., 1993). miRNA derived from the lin4 transcript is a key player in the downregulation of LIN-14, which is necessary for progression from the first larval stage (L1) to L2. In 2001, meiotic silencing by unpaired DNA (MSUD) was discovered in *N. crassa*. MSUD silences genes lacking the paired genes on the homologous chromosome during meiosis (Shiu et al. 2001). miRNA-like RNAs (milRNAs), the first discovered fungal sRNAs similar to miRNAs of plants and animals, were also identified in *N. crassa* (Lee et al., 2010). milRNAs share some features of plant and animal miRNAs, such as the stem-loop structure of the precursor and imperfect complementarity to the target mRNA. Lee et al. also reported milRNAs and Dicer-independent siRNAs (disiRNAs) generated by non-canonical RNAi pathways, which do not require Dicer enzymes. In 2013, it was revealed that fungi could secrete sRNAs into the host plant and hijack the host RNAi machinery to modulate host gene expression (Weiberg et al., 2013).

sRNAs are classified into three classes: siRNAs, microRNAs (miRNAs), and

Piwi-interacting RNAs (piRNAs). These classes mainly differ in terms of their precursor RNAs. The proteins required for sRNA biogenesis and the structures of the AGO-containing complexes also vary among sRNA classes. Accordingly, each sRNA class acquires diverse gene regulation mechanisms and biological roles. siRNAs and miRNAs are 18–25 nucleotides (nt) in length, while piRNAs, which have only been found in animals, are 26–31 nt (Axtell et al., 2011; Ha and Kim, 2014). Generally, siRNAs originate from exogenous factors, such as viruses or transposable elements (TE), and endogenous components, such as transcripts processed by RdRP (Ameres and Zamore, 2013). miRNAs are processed from single-stranded RNA molecules with hairpin structures (Zhuo et al., 2013). These miRNA precursors are located and transcribed individually from the intergenic region, while in metazoans they are often located in the protein-coding region, typically in introns (Axtell et al., 2011; Hinske et al., 2010). Both animals and plants use Dicer to cleave siRNA and miRNA precursors and load them into AGO. However, there are a few different points between animal and plant sRNA biogenesis system. The processing of miRNA precursors requires two cleavages by the RNAse III enzyme. In animals, primary miRNA (pri-miRNA) hairpin is liberated as precursor-miRNA (pre-miRNA) by Drosha in the nucleus, and then the pre-miRNA sequentially subjected to cleavage by Dicer in the cytoplasm (Lam et al., 2015). However, in plants, which do not carry Drosha, the Dicer enzyme conducts the processing of pri- and pre-miRNA in the nucleus (Lam et al., 2015). In case of siRNAs, due to the lack of the stem-loop structure, processing dsRNA into siRNA occurs only via Dicer in both animal and plant system. But the processing of animal siRNAs and plant siRNAs are implemented in the nucleus and the cytoplasm,

respectively (Lam et al., 2015). In fungi, the biogenesis of sRNAs is more similar to the plant system due to the absence of Drosha and piRNAs (Lee et al., 2010). miRNAs often act like programmed gene regulators. Their precursors are transcribed and processed depending on environmental stimuli and developments (Axtell et al., 2011). In contrast, siRNAs typically have roles in genome protection and viral defense (Blair and Olson, 2015). siRNAs generally target repetitive DNA, mRNA with excessive amount, and aberrant RNA (Blair and Olson, 2015; Jorgensen et al., 1996; Lee et al., 2010).

While typical siRNA and miRNA require canonical RNAi components, piRNAs are short single-stranded RNAs generated in non-canonical Dicer-independent pathways. They are found in animal germ cells and are associated with the PIWI subfamily proteins of AGO (Riedmann and Schwentner, 2010). piRNAs suppress repeat elements during germ cell development (Riedmann and Schwentner, 2010). Similar to piRNAs, several siRNA, miRNA, and milRNAs are reportedly generated by non-canonical RNAi pathways, in which Dicer or AGO are not involved (Lee et al., 2010; Yan et al., 2011; Ye et al., 2016). In these cases, the catalytic activity of the AGO family proteins and trimming activity of alternative exonucleases are indispensable for producing mature sRNAs (Lee et al., 2010; Ye et al., 2016). In *Arabidopsis* 3' to 5' exonucleases, Atrimmer 1 and Atrimmer 2 are required for the biogenesis of siRNA independent of Dicer-like (DCL) proteins (sidRNA), which triggers *de novo* DNA methylation of the transposon (Ye et al., 2016). Similarly, primal small RNAs (priRNAs) are generated independently of Dicer and the Triman 3' to 5' exonuclease is required for their production in *Schizosaccharomyces pombe*

(Marasovic et al., 2013). priRNAs induce histone 3 lysine 9 methylation (H3K9me) on centromeric TEs (Marasovic et al., 2013). The generation of Dicer-independent siRNAs (disiRNAs) of *N. crassa* also involves a 3' to 5' exonuclease, ERI-1, as well as DNA methylation on a disiRNA loci where antisense transcriptions occur (Dang et al., 2016). In *Mucor circinelloides*, an RNAase III-like protein, R3B2, is essential for the Dicer-independent production of RdRP-dependent degraded RNA (rdRNA) (Trieu et al., 2015). The R3B2-mediated non-canonical RNA degradation pathway suppresses RNAi-dependent epimutations against antifungal drugs (Calo et al., 2017). Most non-canonical RNAi components are poorly conserved compared to canonical sRNAs, and their functional roles are largely veiled.

RNAi was considered to play a role in the defense against exogenous DNA, including TEs, viruses, and transgenes. However, the scope of its involvement in biological functions, such as genome integrity and gene regulation, has expanded explosively over the past few decades. Recent studies of fungal pathogens described their essential roles in development, stress tolerance, and virulence (Figure 1). This review focused on the experimentally validated roles of RNAi components and sRNA species, to evaluate how fungi exploit RNAi to orchestrate fungal and host physiology, and contribute to virulence.

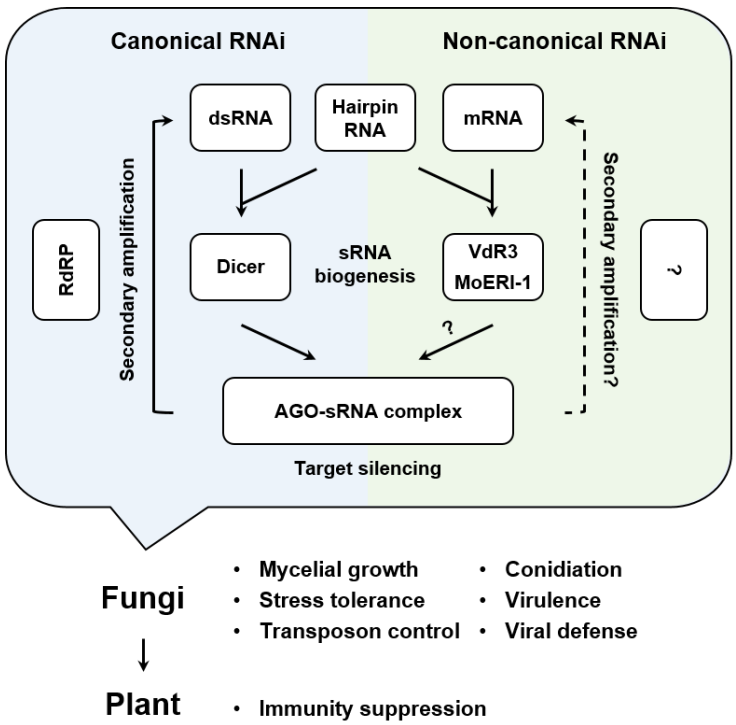


**Figure 1. Schematic overview of RNAi in plant pathogenic fungi.** The corresponding components are shown in each step of canonical and non-canonical RNAi pathway. Since the role of AGO in the silencing step has not been experimentally proved in plant pathogenic fungi, the formation of AGO-sRNA complex is indicated with a question mark. Secondary amplification and related component are also indicated with question marks, as they have not been reported in non-canonical RNAi of fungi. The roles of endogenous RNAi and cross-kingdom RNAi are shown below. AGO, Argonaute; RdRP, RNA-dependent RNA polymerase.

# I. Roles of RNAi in fungal development and pathogenesis

Many important crops are invaded by pathogenic fungi, which causes worldwide economic yield losses every year. Therefore, there is a need for alternative infection control methods and a more profound understanding of the involvement of RNAi in fungal pathogenesis. The RNAi components of many plant pathogenic fungi have been functionally investigated and shown to be involved in the pathogenesis or related biological processes of fungi. *Botrytis cinerea*, *Magnaporthe oryzae*, *Fusarium oxysporum* f. sp. *cubense*, and *Colletotrichum gloeosporioides* actively utilize RNAi pathways for mycelial growth, conidiation, and virulence (Table 1). Mutants lacking one or two RNAi components in those species showed no, or decreased, ability to infect the host tissues (Li et al., 2022; Raman et al., 2017; Wang et al., 2018; Weiberg et al., 2013). Similar to Dicer proteins of the model fungus *N. crassa* which showed functional redundancy, those of *B. cinerea* and *C. gloeosporioide* have redundant functions in the fungal pathogenesis (Catalanotto et al., 2004; Wang et al., 2018; Weiberg et al., 2013). In contrast, *M. oryzae* and *F. oxysporum* f. sp. *cubense* DCL2 proteins, rather than DCL1, are primarily involved in virulence (Li et al., 2022; Raman et al., 2017; Zanini et al., 2021). Dicer and AGO2 mutants of *Sclerotinia sclerotiorum* and *Valsa mali* showed reduced mycelial growth and virulence (Feng et al., 2017a; Feng et al., 2017b; Mochama, 2018a; Mochama et al., 2018b; Yang et al., 2021). While the Dicer proteins *S. sclerotiorum* showed redundancy under all conditions tested, those of *V. mali* were redundant only in the context of oxidative stress responses (Feng et al., 2017a; Mochama, 2018a). *VmDCL2*, but not *VmDCL1*, was involved in the virulence of *V. mali* (Feng et al.,

2017a). *Fusarium graminearum* also showed distinct redundancies according to biological processes. Both deleting FgDICER1 and FgDICER2 decreased virulence on barley and *Brachypodium distachyon*, whereas deleting FgDICER2 and FgAGO2, but not FgDICER1, reduced forcible ascospore discharge (Son et al., 2017; Werner et al., 2021). Experimental investigation of the RNAi components in *Penicillium italicum*, *Zymoseptoria tritici*, *F. oxysporum* f. sp. *lycopersici*, and *Verticillium dahliae* revealed their relevance to fungal virulence, but not to other conditions (Habig et al., 2021; Jo et al., 2018; Yin et al., 2020). The virulence of the *Pit-DCL2*-silenced mutant to citrus fruits was severely impaired compared to that of the *Pit-DCL1* and the wild type in *P. italicum,* while silencing *VdDCL1* and *VdDCL2* by external RNAs reduced the impact of wilt disease caused by *V. dahliae* (Yin et al., 2020). In *Z. tritici*, deleting *ZtAGO1* reduced the ability to produce asexual propagules *in planta* (Habig et al., 2021). *F. oxysporum* f. sp. *lycopersici* contains four homologs of *QDE-2* (*AGO2*) of *N. carassa*, two of them were characterized, and from the two, one AGO2 protein, FoQDE2, had a role only in fungal virulence (Jo et al., 2018).

Non-canonical RNAi components also participate in fungal pathogenesis. In *V. dahliae*, the VdR3 RNAseIII domain-containing protein is crucial for the biogenesis of VdmilR1, which targets *VdHy1* (Jin et al., 2019). The *VdHy1* deletion mutant exhibited reduced mycelial growth and melanin production and could not induce wilt symptoms in cotton plants (Jin et al., 2019). In addition, the non-canonical RNAi pathway plays an important role in the conidiation of fungi. In *N. crassa*, disiRNA and the ERI-1 exonuclease regulated circadian clock gene *frequency* (*frq*) and

conidiation (Dang et al., 2016). Deletion mutant of *MoERI*-1, a *ERI-1* homologue in *M. oryzae*, showed reduced mycelial growth, abnormal septa formation, and increased conidiation (Lee et al., 2022). In addtion, the deletion of *MoERI-1* caused decrease of *MoERI-1*-dependent sRNAs and increase of mRNA transcripts from conidiation-related genes (Lee et al., 2022).

**Table 1. RNAi core components characterized in plant pathogenic fungi**

| Species | Characterized RNAi component | Related phenotypes/mechanism | Reference |
|---|---|---|---|
| *Fusarium graminearum* | FgDICER1 | Conidiation, sexual development, virulence /antiviral defense | Son et al., 2017; Yu et al. 2018; Zheng et al., 2018; Gaffaer et al., 2019; Werner et al., 2021 |
| | FgDICER2 | Conidiation, sexual development, virulence /antiviral defense | Gaffaer et al., 2019; Werner et al., 2021 |
| | FgAGO1 | Conidiation, sexual development, virulence /antiviral defense | Son et al., 2017; Yu et al. 2018; Zheng et al., 2018; Gaffaer et al., 2019; Werner et al., 2021 |
| | FgAGO2 | Sexual development, virulence /antiviral defense | Son et al., 2017; Gaffaer et al., 2019 |
| | FgRDR1 | Sexual development, virulence | Son et al., 2017; Gaffaer et al., 2019 |
| | FgRDR2 | Conidiation, sexual development, virulence | Gaffaer et al., 2019; Werner et al., 2021 |
| | FgRDR3 | Conidiation, sexual development, virulence | Gaffaer et al., 2019; Werner et al., 2021 |
| | FgRDR4 | Conidiation, sexual development, virulence | Gaffaer et al., 2019; Werner et al., 2021 |
| | FgRDR5 | Antiviral defense | Chen et al., 2015 |
| *Magnaporthe oryzae* | MoDCL1 | Conidiation, virulence | Raman et al., 2017; Zanini et al., 2021 |
| | MoDCL2 | Mycelial growth, conidiation /transposon control | Kadotani et al., 2004; Murata et al., 2007; Raman et al., 2017; Zanini et al., 2021 |
| | MoAGO1 | Conidiation /antiviral defense, transposon control | Raman et al., 2017; Nguyen et al., 2018 |

| | | | |
|---|---|---|---|
| | MoAGO2 | Conidiation, virulence /antiviral defense, transposon control | Raman et al., 2017; Zanini et al., 2021 |
| | MoAGO3 | Mycelial growth, conidiation, virulence /antiviral defense, transposon control | Raman et al., 2017; Nguyen et al., 2018 |
| | MoRdRP1 | Mycelial growth, conidiation, virulence | Raman et al., 2017 |
| | MoRdRP2 | Conidiation | Raman et al., 2017 |
| | MoRdRP3 | Conidiation | Raman et al., 2017 |
| *Valsa mali* | VmDCL1 | Stress tolerance | Feng et al., 2017a |
| | VmDCL2 | Stress tolerance, virulence /antiviral defense | Feng et al., 2017a; Yang et al., 2021 |
| | VmAGO2 | Mycelial growth, stress tolerance, virulence | Feng et al., 2017b |
| *Sclerotinia sclerotiorum* | dcl-1 | Mycelial growth, virulence /antiviral defense | Mochama et al., 2018a |
| | dcl-2 | Mycelial growth, virulence /antiviral defense | Mochama et al., 2018a |
| | ago-2 | Mycelial growth, virulence /antiviral defense | Mochama et al., 2018a |
| *Fusarium oxysporum* f. sp. *cubense* | FoDCL1 | Conidiation | Li et al., 2022 |
| | FoDCL2 | Virulence | Li et al., 2022 |
| | FoQDE2 (AGO2) | Mycelial growth, conidiation, stress tolerance, virulence | Li et al., 2022 |
| *Botrytis cinerea* | Bc-DCL1 | Mycelial growth, conidiation, virulence | Weiberg et al., 2013 |
| | Bc-DCL2 | Mycelial growth, conidiation, virulence | Weiberg et al., 2013 |
| *Cryphonectria parasitica* | DCL2 | Antiviral defense | Segers et al., 2007 |
| | AGL2 | Antiviral defense | Sun et al., 2009 |
| *Colletotrichum higginsianum* | DCL1 | Antiviral defense | Campo et al., 2016 |
| | AGO1 | Antiviral defense | Campo et al., 2016 |
| *Colletotrichum gloeosporioides* | Dcl1 | Mycelial growth, conidiation, virulence | Wang et al., 2018a |
| | Dcl2 | Mycelial growth, conidiation, virulence | Wang et al., 2018a |

| | | | |
|---|---|---|---|
| *Verticillium dahliae* | VdDCL1 | Virulence | Wang et al., 2018b |
| | VdDCL2 | Virulence | Wang et al., 2018b |
| *Fusarium oxysporum* f. sp. *lycopersici* | FoQDE2 (AGO2) | Virulence | Jo et al., 2018 |
| *Penicillium italicum* | Pit-DCL2 | Virulence | Yin et al., 2020 |
| *Zymoseptoria tritici* | ZtAGO1 | Virulence | Habig et al., 2021 |

## II. Anti-viral roles of RNAi

Plants, flies, worms, and fungi use the RNAi machinery as an innate immune system to defend against invading viruses (Segers et al., 2007; Zhou and Rana, 2013). In plant pathogenic fungi, viral defense by RNAi contributes to full fungal virulence (Sun et al., 2009; Zhang et al., 2008; Campo et al., 2016). Therefore, understanding the innate antiviral mechanisms of plant pathogenic fungi against mycoviruses is essential to apply mycoviruses as biological reagents against fungal pathogens. The role of RNAi in the antiviral defense mechanism of fungi was first reported in the causal agent of chestnut blight, *Cryphonectria parasitica* (Segers et al., 2007). *C. parasitica* uses dcl2 and agl2 to coordinate inducible antiviral responses against the mycovirus, *Cryphonectria* hypovirus 1 (CHV1) (Sun et al., 2009; Zhang et al., 2008). RNAi is also essential in the antiviral defense of *M. oryzae* (Nguyen et al., 2018). MoAGO3 and MoDCL2 suppress viral RNAs of PoOLV1 and PoOLV2, respectively. Intriguingly, MoAGO2 interferes with RNAi by competing with MoAGO3 to bind a similar sRNA pool. Deleting MoAGO3 increased viral RNA, while deleting MoAGO2 reduced it. In *F. graminearum*, FgDICER1, FgDICER2, FgAGO1, and FgAGO2 suppress viral RNAs redundantly (Yu et al., 2018). In addition, FgDICER2 has a major role in the defense against viroids (Wei et al., 2019). Introducing the hop stunt viroid (HSVd) into the FgDICER2 deletion mutant resulted in increased HSVd RNA levels and reductions in mycelial growth and virulence in maize seedlings. Similarly, two RNAi components, dcl1 and ago1, are crucial for the antiviral response of the plant pathogenic fungus *Colletotrichum higginsianum*. Deletion of these genes increased the accumulation of the novel dsRNA virus, *Colletotrichum*

*higginsianum* nonsegmented dsRNA virus 1 (ChNRV1) (Campo et al., 2016). The severe defects in conidiation and conidia morphology seen for dcl1 and ago1 deletion mutants resulted from increased viral RNAs , indicating that RNAi suppressed the viruses and their injurious effects.

Those results reported in *C. higginsianum* implied a notable issue. The deletion mutants of RNAi components in *C. higginsianum* showed changes in phenotypes, but those alterations resulted from the increased viral RNA, not from the disruption of regulatory function toward endogenous genes. Thus, it is necessary to examine the effect of the mycoviral infection in the process of functional characterization of RNAi components. In addition, the effect of mycoviral infection might explain the phenotypic diversity between different strains or isolates in plant pathogenic fungi. For example, in *M. oryzae*, functional studies of Dicer genes have been conducted in three different strains. Mutants of same *MoDCL* genes originating from different stain/isolate backgrounds presented diverse phenotypic changes including decreases of mycelial growth, conidiation, virulence, and ability to suppress transposons (Kadotani et al., 2004; Raman et al., 2017; Zanini et al., 2021; Lee et al., 2022). Similar cases were also found in the functional characterization studies of RNAi components in *F. graminearum* (Chen et al., 2015; Son et al., 2017; Yu et al. 2018; Zheng et al., 2018; Gaffaer et al., 2019; Werner et al., 2021). Given that there are few sequence variations in RNAi components between strains/isolates, it is possible that the phenotypic diversity of RNAi mutants might be caused by whether a particular mycovirus is infected.

## III. Control of transposable element by RNAi

TEs are DNA sequences capable of changing position within a genome. They have roles in centromere function, genome reorganization, and gene expression regulation (Diehl et al., 2020; Hirsch and Springer, 2017; Klein and O'Neill, 2018). Many organisms have developed mechanisms to control TE activity (Castanera et al., 2016; Friedli and Trono, 2015). The RNAi functions in TE repression have been well characterized in animals, plants, and other organisms (Aravin et al., 2001; Bourc'his and Voinnet, 2010; Sijen and Plasterk, 2003). RNAi mechanisms for TE regulation have also been studied in plant pathogenic fungi. In the rice blast fungus *M. oryzae*, approximately 70% of all sRNAs detected in the mycelial stage mapped to repetitive DNA and LTR-retrotransposons, and RNAi components controlled the LTR-retrotransposon MAGGY (Lee et al., 2022; Raman et al., 2013; Raman et al., 2017). Similar to viral defense, MoAGO1 and MoAGO3 negatively control MAGGY, whereas MoAGO2 positively regulates MAGGY transcript levels (Nguyen et al., 2018). These results reflect efforts to maintain proper TE transcript levels to achieve an evolutionary advantage, including genome reorganization and gene birth/removal.

Effector proteins are used by filamentous pathogens to overcome unfavorable environments in host plants. Host plants exploit resistance proteins to recognize effectors. Many effector genes in fungal pathogens, such as *M oryzae* and *Leptosphaeria maculans*, are in close proximity to repetitive elements like TEs (Fahlgren et al., 2013; Kim et al., 2019). TE-derived sRNAs are hypothesized to control TEs and nearby effector genes through heterochromatin formation (Whisson

et al., 2012). However, more experimental evidence is required to elucidate the role of TE-derived sRNA in regulating effector genes.

## IV. Characterized sRNAs in plant pathogenic fungi

Several fungal endogenous sRNAs that participate in the fine-tuning of pathogenicity-related genes have been functionally characterized (Table 2). In *F. graminearum*, *Fg*-milR2 regulates the expression of *FgbioH1*, which is required for mycelial growth, virulence, and mycotoxin biosynthesis (Guo et al., 2019). *F. oxysporum* f. sp. *cubense* exploited milR-87 to regulate a glycosyl hydrolase-coding gene, *FOIG_15013* (Li et al., 2022). Overexpression of milR-87 led to an increase in mycelial growth, conidiation, and virulence. *M. oryzae* produces milR236 which targets *MoHat1* (a histone acetyltransferase type B catalytic subunit coding gene) (Li et al., 2020). Overexpression of milR236 delays appressorium formation and virulence attenuation. *VdMILR1* from *V. dahliae* induces transcriptional repression by increasing histone H3K9 methylation of *VdHy1*, which is essential for fungal virulence (Jin et al., 2019). In the apple tree Valsa canker pathogen, *V. mali*, *Vm*-milR16 targets three genes essential for the oxidative stress response: *VmSNF1, VmDODA,* and *VmHY1* (Xu et al., 2020). Overexpression of Vm-milR16 and deletion of three target genes reduced the virulence. Likewise, overexpression of Vm-milR37 abolished the pathogenicity by targeting a glutathione peroxidase gene, *VmGP*, which is crucial for tolerance to oxidative stress (Feng et al., 2021). Expression profiling revealed that *Vm*-milR37 was expressed in the mycelium, but

not during infection. This indicates that *Vm*-milR37 suppresses pathogenicity-related genes during the vegetative stage. Another *V. mali* milRNA, *Vm*-PC-3p-921076, degrades the transcript of *Vm-VPS10*, which is essential for mycelial growth and fungal virulence (Guo et al., 2021). Moreover, deletion and overexpression of *Vm*-PC-3p-921076 increased and decreased virulence, respectively.

Pathogen-derived sRNAs can be transferred into host cells to mediate the suppression of host immunity. Because these cross-kingdom sRNAs are secreted and modulate host physiology, they have also been called "sRNA effectors". The first fungal sRNA effectors were found in *B. cinerea* (Weiberg et al., 2013). Most *B. cinerea* sRNA effectors are derived from long terminal repeat (LTR) retrotransposons and bind to *Arabidopsis* AGO1, thereby silencing the host immunity genes. Meanwhile, *Bc*-siR37 originated from the gene-coding region (Wang et al., 2017). *Bc*-siR37 differs from other reported *B. cinerea* sRNA effectors in that it can target multiple host genes. *Bc*-siR37 suppresses at least 15 *Arabidopsis* genes, including receptor-like kinases, WRKY transcription factors, and cell wall-modifying enzymes. The wheat pathogen *Puccinia striiformis* f. sp. *tritici* also secretes *Pst*-milR1 into host cells and silences the defense-related gene *TaPR2* (Wang et al., 2017). Silencing of the Pst-milR1 precursor enhanced the resistance of wheat against a virulent *Pst* isolate. *F. oxysporum* f. sp. *lycopersici* exports *Fol*-milR1 into tomato, targeting the CBL-interacting protein kinase gene *SlyFRG4* (Ji et al., 2021). Deletion and overexpression of *Fol*-milR1 attenuated and enhanced virulence, respectively. Like *B. cinerea* sRNA effectors, *Fol*-milR1 also hijacks the host RNAi machinery by binding to tomato AGO4. In *V. mali*, a milRNA *Vm*-milR1

was induced during infection, and deleting *Vm*-milR1 reduced the virulence (Xu et al., 2022). *Vm*-milR1 suppresses the expression of two host receptor-like kinase genes, *MdRLKT1* and *MdRLKT2*, the knockdown of which compromised host resistance to *V. mali*. A recent study of *V*. *dahliae* sRNAs revealed a unique sRNA effector, *Vd*rsR-1 (Zhang et al., 2022). *Vd*rsR-1 is secreted into *Arabidopsis* and targets a host miRNA precursor of miR157d, resulting in increased accumulation of miR157d. This up-regulation of miR157d suppresses *SPL13A/B*, thereby retarding plant floral transition and prolonging the host vegetative growth, which enhances fungal propagation.

**Table 2. Identified sRNAs with validated targets and functions**

| Species | Small RNA | Target organism | Target gene | Related phenotypes | Reference |
|---|---|---|---|---|---|
| *Valsa mali* | *Vm*-milR16 | *V. mali* | *VmSNF1, VmDODA, VmHY1* | Mycelial growth, stress tolerance, virulence | Xu et al., 2020 |
| | *Vm*-milR37 | *V. mali* | *VmGP* | Stress tolerance, virulence | Feng et al., 2020 |
| | *Vm*-PC-3p-921076 | *V. mali* | *Vm-VPS10* | Mycelial growth, virulence | Guo et al., 2021 |
| | *Vm*-milR1 | *Malus domestica* | *MdRLKT1, MdRLKT2* | Virulence | Xu et al., 2021 |
| *Botrytis cinerea* | *Bc*-siR3.1 | *Arabidopsis thaliana* | *AtMPK1, AtMPK2* | Virulence | Weiberg et al., 2013 |
| | *Bc*-siR3.2 | *A. thaliana* | *AtPRXIIF* | Virulence | Weiberg et al., 2013 |
| | *Bc*-siR5 | *A. thaliana* | *AtWAK* | Virulence | Weiberg et al., 2013 |
| | *Bc*-siR37 | *A. thaliana* | *AtWRKY7, AtFEI2, AtPRM6* | Virulence | Wang et al., 2017 |
| *Verticillium dahliae* | *Vd*-milR1 | *V. dahliae* | *VdHY1* | Mycelial growth, virulence | Jin et al., 2019 |
| | *Vd*rsR-1 | *A. thaliana* | *miR157d* | Stunting and delayed floral transition | Zhang et al., 2022 |
| *Rhizoctonia solani* | *Rhi*-milR-16 | *R. solai* | *AG1IA_02173* | Unknown | Lin et al., 2016 |
| *Fusarium graminearum* | *Fg*-milR2 | *F. graminearum* | *FgbioH1* | Mycelial growth, virulence | Guo et al., 2019 |

| | | | | | |
|---|---|---|---|---|---|
| *Magnaporthe oryzae* | *Mo*-milR236 | *M. oryzae* | *MoHAT1* | Virulence | Yang et al., 2020 |
| *Fusarium oxysporum* f. sp. *cubense* | milR-87 | *F. oxysporum* f. sp. *Cubense* | *FOIG_15013* | Mycelial growth, conidiation, stress tolerance, virulence | Li et al., 2022 |
| *Puccinia striiformis* f. sp. *Tritici* | *Pst*-milR1 | *Triticum aestivum* | *TaPR2* | Virulence | Wang et al., 2017 |
| *Fusarium oxysporum* f. sp. *lycopersici* | *Fol*-milR1 | *Solanum lycopersicum* | *SlyFRG4* | Virulence | Ji et al., 2021 |

# Conclusion

The development of molecular genetic tools and the accumulation of sRNA profiles led to the characterization of RNAi components and the discovery of various sRNAs in plant pathogenic fungi. RNAi contributes to survival and pathogenesis of fungal pathogens by fungal developments, stress tolerance, antiviral defense, and transposon control. Beyond regulating endogenous pathogenesis-related genes, fungi also deploy RNAi front lines of the battle field by secreting sRNAs to hijack host RNAi machinery. It is clear that plant pathogenic fungi exploit RNAi in various ways to fine-tune the disease development. Moreover, the contributions of non-canonical RNAi pathway in plant pathogenesis, which have just begun to be discovered, suggest that vast territories of RNAi functions in plant pathogenic fungi remain veiled.

# LITERATURE CITED


Ameres, SL and Zamore, PD 2013. Diversifying microRNA sequence and function. *Nat. Rev. Mol. Cell Biol.* 14: 475-488.

Aravin, AA, Naumova, NM, Tulin, AV, Vagin, VV, Rozovsky, YM and Gvozdev, VA 2001. Double-stranded RNA-mediated silencing of genomic tandem repeats and transposable elements in the *D. melanogaster* germline. *Curr. Biol.* 11: 1017-1027.

Åsman, AK, Fogelqvist, J, Vetukuri, RR and Dixelius, C 2016. *Phytophthora infestans* Argonaute 1 binds micro RNA and small RNA s from effector genes and transposable elements. *New Phytol.* 211: 993-1007.

Axtell, MJ, Westholm, JO and Lai, EC 2011. Vive la différence: biogenesis and evolution of microRNAs in plants and animals. *Genome Biol.* 12: 1-13.

Blair, CD and Olson, KE 2015. The role of RNA interference (RNAi) in arbovirus-vector interactions. *Viruses* 7: 820-843.

Bourc'his, D and Voinnet, O 2010. A small-RNA perspective on gametogenesis, fertilization, and early zygotic development. *Science* 330: 617-622.

Chow, FW-N, Koutsovoulos, G, Ovando-Vázquez, C, Neophytou, K, Bermúdez-Barrientos, JR, Laetsch, DR, Robertson, E, Kumar, S, Claycomb, JM and Blaxter, M 2019. Secretion of an Argonaute protein by a parasitic nematode and the evolution of its siRNA guides. *Nucleic Acids Res.* 47: 3594-3606.

Cai, Q, Qiao, L, Wang, M, He, B, Lin, F-M, Palmquist, J, Huang, S-D and Jin, H 2018. Plants send small RNAs in extracellular vesicles to fungal pathogen to silence virulence genes. *Science* 360: 1126-1129.

Calo, S, Nicolas, FE, Lee, SC, Vila, A, Cervantes, M, Torres-Martinez, S, Ruiz-Vazquez, RM, Cardenas, ME and Heitman, J 2017. A non-canonical RNA degradation pathway suppresses RNAi-dependent epimutations in the human fungal pathogen *Mucor circinelloides*. *PLoS Genet.* 13: e1006686.

Campo, S, Gilbert, KB and Carrington, JC 2016. Small RNA-based antiviral defense in the phytopathogenic fungus *Colletotrichum higginsianum*. *PLoS Path.* 12: e1005640.

Castanera, R, Lopez-Varas, L, Borgognone, A, LaButti, K, Lapidus, A, Schmutz, J, Grimwood, J, Perez, G, Pisabarro, AG and Grigoriev, IV 2016. Transposable elements versus the fungal genome: impact on whole-genome architecture and transcriptional profiles. *PLoS Genet.* 12: e1006108.

Catalanotto, C, Pallotta, M, ReFalo, P, Sachs, MS, Vayssie, L, Macino, G and Cogoni, C 2004. Redundancy of the two dicer genes in transgene-induced posttranscriptional gene silencing in *Neurospora crassa*. *Mol. Cell. Biol.* 24: 2536-2545.

Cogoni, C and Macino, G 1999. Gene silencing in *Neurospora crassa* requires a protein homologous to RNA-dependent RNA polymerase. *Nature* 399: 166-169.

Dang, Y, Cheng, J, Sun, X, Zhou, Z and Liu, Y 2016. Antisense transcription licenses nascent transcripts to mediate transcriptional gene silencing. *Genes Dev.* 30: 2417-2432.

Diehl, AG, Ouyang, N and Boyle, AP 2020. Transposable elements contribute to cell and species-specific chromatin looping and gene regulation in mammalian genomes. *Nat. Commun.* 11: 1-18.

Fahlgren, N, Bollmann, SR, Kasschau, KD, Cuperus, JT, Press, CM, Sullivan, CM, Chapman, EJ, Hoyer, JS, Gilbert, KB and Grünwald, NJ 2013. Phytophthora have distinct endogenous small RNA populations that include short interfering and microRNAs. *PLoS One* 8: e77181.

Feng, H, Xu, M, Liu, Y, Dong, R, Gao, X and Huang, L 2017. Dicer-Like Genes Are Required for H2O2 and KCl Stress Responses, Pathogenicity and Small RNA Generation in *Valsa mali*. *Front Microbiol* 8: 1166.

Feng, H, Xu, M, Liu, Y, Gao, X, Yin, Z, Voegele, R and Huang, L 2017. The distinct roles of Argonaute protein 2 in the growth, stress responses and pathogenicity of the apple tree canker pathogen. *For. Pathol.* 47: e12354.

Feng, H, Xu, M, Gao, Y, Liang, J, Guo, F, Guo, Y and Huang, L 2021. Vm-milR37 contributes to pathogenicity by regulating glutathione peroxidase gene VmGP in *Valsa mali*. *Mol. Plant Pathol.* 22: 243-254.

Fire, A, Xu, S, Montgomery, MK, Kostas, SA, Driver, SE and Mello, CC 1998. Potent and specific genetic interference by double-stranded RNA in

*Caenorhabditis elegans*. *Nature* 391: 806-811.

Friedli, M and Trono, D 2015. The developmental control of transposable elements and the evolution of higher species. *Annu. Rev. Cell. Dev. Biol.* 31: 429-451.

Guo, F, Liang, J, Xu, M, Zhang, G, Huang, L and Feng, H 2021. A Novel DCL2-Dependent Micro-Like RNA Vm-PC-3p-92107_6 Affects Pathogenicity by Regulating the Expression of Vm-VPS10 in *Valsa mali*. *Front. Microbiol.* 2779.

Guo, MW, Yang, P, Zhang, JB, Liu, G, Yuan, QS, He, WJ, Nian, JN, Yi, SY, Huang, T and Liao, YC 2019. Expression of microRNA-like RNA-2 (Fgmil-2) and bioH1 from a single transcript in *Fusarium graminearum* are inversely correlated to regulate biotin synthesis during vegetative growth and host infection. *Mol. Plant Pathol.* 20: 1574-1581.

Ha, M and Kim, VN 2014. Regulation of microRNA biogenesis. *Nat. Rev. Mol. Cell Biol.* 15: 509-524.

Habig, M, Schotanus, K, Hufnagel, K, Happel, P and Stukenbrock, EH 2021. Ago1 affects the virulence of the fungal plant pathogen *Zymoseptoria tritici*. *Genes* 12: 1011.

Hammond, SM, Bernstein, E, Beach, D and Hannon, GJ 2000. An RNA-directed nuclease mediates post-transcriptional gene silencing in *Drosophila* cells. *Nature* 404: 293-296.

He, B, Cai, Q, Qiao, L, Huang, C-Y, Wang, S, Miao, W, Ha, T, Wang, Y and Jin, H

2021. RNA-binding proteins contribute to small RNA loading in plant extracellular vesicles. *Nat. plants* 7: 342-352.

Hinske, LCG, Galante, PA, Kuo, WP and Ohno-Machado, L 2010. A potential role for intragenic miRNAs on their hosts' interactome. *BMC Genom.* 11: 1-13.

Hirsch, CD and Springer, NM 2017. Transposable element influences on gene expression in plants. *Biochim. Biophys. Acta Gene Regul. Mech.* 1860: 157-165.

Ji, HM, Mao, HY, Li, SJ, Feng, T, Zhang, ZY, Cheng, L, Luo, SJ, Borkovich, KA and Ouyang, SQ 2021. Fol-milR1, a pathogenicity factor of *Fusarium oxysporum*, confers tomato wilt disease resistance by impairing host immune responses. *New Phytol.* 232: 705-718.

Jin, Y, Zhao, J-H, Zhao, P, Zhang, T, Wang, S and Guo, H-S 2019. A fungal milRNA mediates epigenetic repression of a virulence gene in *Verticillium dahliae*. *Philos. Trans. R. Soc. Lond., B, Biol. Sci.* 374: 20180309.

Jo, S-M, Ayukawa, Y, Yun, S-H, Komatsu, K and Arie, T 2018. A putative RNA silencing component protein FoQde-2 is involved in virulence of the tomato wilt fungus *Fusarium oxysporum* f. sp. *lycopersici*. *J. Gen. Plant Pathol.* 84: 395-398.

Jorgensen, RA, Cluster, PD, English, J, Que, Q and Napoli, CA 1996. Chalcone synthase cosuppression phenotypes in petunia flowers: comparison of sense vs. antisense constructs and single-copy vs. complex T-DNA sequences.

*Plant Mol. Biol.* 31: 957-973.

Kim, K-T, Ko, J, Song, H, Choi, G, Kim, H, Jeon, J, Cheong, K, Kang, S and Lee, Y-H 2019. Evolution of the genes encoding effector candidates within multiple pathotypes of *Magnaporthe oryzae*. *Front. Microbiol* 10: 2575.

Klein, SJ and O'Neill, RJ 2018. Transposable elements: genome innovation, chromosome diversity, and centromere conflict. *Chromosome Res.* 26: 5-23.

Lam, JK, Chow, MY, Zhang, Y and Leung, SW 2015. siRNA versus miRNA as therapeutics for gene silencing. *Mol. Ther. Nucleic Acids* 4: e252.

Lee, H-C, Aalto, AP, Yang, Q, Chang, S-S, Huang, G, Fisher, D, Cha, J, Poranen, MM, Bamford, DH and Liu, Y 2010. The DNA/RNA-dependent RNA polymerase QDE-1 generates aberrant RNA and dsRNA for RNAi in a process requiring replication protein A and a DNA helicase. *PLoS Biol.* 8: e1000496.

Lee, H-C, Li, L, Gu, W, Xue, Z, Crosthwaite, SK, Pertsemlidis, A, Lewis, ZA, Freitag, M, Selker, EU and Mello, CC 2010. Diverse pathways generate microRNA-like RNAs and Dicer-independent small interfering RNAs in fungi. *Mol. Cell* 38: 803-814.

Lee, H, Choi, G, Lim, Y-J and Lee, Y-H 2022. Comparative profiling of canonical and non-canonical small RNAs in the rice blast fungus, *Magnaporthe oryzae*. *Front. Microbiol*: 3657.

Lee, RC, Feinbaum, RL and Ambros, V 1993. The C. elegans heterochronic gene

lin-4 encodes small RNAs with antisense complementarity to lin-14. *Cell* 75: 843-854.

Li, M, Xie, L, Wang, M, Lin, Y, Zhong, J, Zhang, Y, Zeng, J, Kong, G, Xi, P and Li, H 2022. FoQDE2-dependent milRNA promotes *Fusarium oxysporum* f. sp. *cubense* virulence by silencing a glycosyl hydrolase coding gene expression. *PLoS Path.* 18: e1010157.

Li, Y, Liu, X, Yin, Z, You, Y, Zou, Y, Liu, M, He, Y, Zhang, H, Zheng, X and Zhang, Z 2020. MicroRNA-like milR236, regulated by transcription factor MoMsn2, targets histone acetyltransferase MoHat1 to play a role in appressorium formation and virulence of the rice blast fungus *Magnaporthe oryzae*. *Fungal Genet. Biol.* 137: 103349.

Marasovic, M, Zocco, M and Halic, M 2013. Argonaute and Triman generate dicer-independent priRNAs and mature siRNAs to initiate heterochromatin formation. *Mol. Cell* 52: 173-183.

Mochama, P 2018. Dissecting RNA Silencing Pathways in *Sclerotinia Sclerotiorum*. *Electronic Theses and Dissertations*. 2635.

Mochama, P, Jadhav, P, Neupane, A and Lee Marzano, S-Y 2018. Mycoviruses as triggers and targets of RNA silencing in white mold fungus *Sclerotinia sclerotiorum*. *Viruses* 10: 214.

Napoli, C, Lemieux, C and Jorgensen, R 1990. Introduction of a chimeric chalcone synthase gene into petunia results in reversible co-suppression of

homologous genes in trans. *The plant cell* 2: 279-289.

Nguyen, Q, Iritani, A, Ohkita, S, Vu, BV, Yokoya, K, Matsubara, A, Ikeda, K-i, Suzuki, N and Nakayashiki, H 2018. A fungal Argonaute interferes with RNA interference. *Nucleic Acids Res.* 46: 2495-2508.

Qutob, D, Patrick Chapman, B and Gijzen, M 2013. Transgenerational gene silencing causes gain of virulence in a plant pathogen. *Nat. commun.* 4: 1-6.

Raman, V, Simon, SA, Romag, A, Demirci, F, Mathioni, SM, Zhai, J, Meyers, BC and Donofrio, NM 2013. Physiological stressors and invasive plant infections alter the small RNA transcriptome of the rice blast fungus, *Magnaporthe oryzae*. *BMC Genom.* 14: 1-18.

Raman, V, Simon, SA, Demirci, F, Nakano, M, Meyers, BC and Donofrio, NM 2017. Small RNA Functions Are Required for Growth and Development of *Magnaporthe oryzae*. *Mol. Plant Microbe. Interact.* 30: 517-530.

Riedmann, LT and Schwentner, R: miRNA, siRNA, piRNA and argonautes: news in small matters. *Taylor & Francis*; 2010.

Romano, N and Macino, G 1992. Quelling: transient inactivation of gene expression in *Neurospora crassa* by transformation with homologous sequences. *Mol. Microbiol.* 6: 3343-3353.

Segers, GC, Zhang, X, Deng, F, Sun, Q and Nuss, DL 2007. Evidence that RNA silencing functions as an antiviral defense mechanism in fungi. *Proc. Natl. Acad. Sci.* 104: 12902-12906.

Sijen, T and Plasterk, RH 2003. Transposon silencing in the *Caenorhabditis elegans* germ line by natural RNAi. *Nature* 426: 310-314.

Son, H, Park, AR, Lim, JY, Shin, C and Lee, YW 2017. Genome-wide exonic small interference RNA-mediated gene silencing regulates sexual reproduction in the homothallic fungus *Fusarium graminearum*. *PLoS Genet.* 13: e1006595.

Sun, Q, Choi, GH and Nuss, DL 2009. A single Argonaute gene is required for induction of RNA silencing antiviral defense and promotes viral RNA recombination. *Proc. Natl. Acad. Sci.* 106: 17927-17932.

Trieu, TA, Calo, S, Nicolas, FE, Vila, A, Moxon, S, Dalmay, T, Torres-Martinez, S, Garre, V and Ruiz-Vazquez, RM 2015. A non-canonical RNA silencing pathway promotes mRNA degradation in basal Fungi. *PLoS Genet.* 11: e1005168.

Vetukuri, RR, Åsman, AK, Tellgren-Roth, C, Jahan, SN, Reimegård, J, Fogelqvist, J, Savenkov, E, Söderbom, F, Avrova, AO and Whisson, SC 2012. Evidence for small RNAs homologous to effector-encoding genes and transposable elements in the oomycete *Phytophthora infestans*. *PloS one* 7: e51399.

Wang, B, Sun, Y, Song, N, Zhao, M, Liu, R, Feng, H, Wang, X and Kang, Z 2017. *Puccinia striiformis* f. sp. *tritici* microRNA-like RNA 1 (Pst-milR1), an important pathogenicity factor of *Pst*, impairs wheat resistance to *Pst* by suppressing the wheat pathogenesis-related 2 gene. *New Phytol.* 215: 338-350.

Wang, L, Xu, X, Yang, J, Chen, L, Liu, B, Liu, T and Jin, Q 2018. Integrated microRNA and mRNA analysis in the pathogenic filamentous fungus *Trichophyton rubrum*. *BMC Genom.* 19: 933.

Wang, M, Weiberg, A, Dellota Jr, E, Yamane, D and Jin, H 2017. *Botrytis* small RNA Bc-siR37 suppresses plant defense genes by cross-kingdom RNAi. *RNA Biol.* 14: 421-428.

Wei, S, Bian, R, Andika, IB, Niu, E, Liu, Q, Kondo, H, Yang, L, Zhou, H, Pang, T and Lian, Z 2019. Symptomatic plant viroid infections in phytopathogenic fungi. *Proc. Natl. Acad. Sci.* 116: 13042-13050.

Weiberg, A, Wang, M, Lin, F-M, Zhao, H, Zhang, Z, Kaloshian, I, Huang, H-D and Jin, H 2013. Fungal small RNAs suppress plant immunity by hijacking host RNA interference pathways. *Science* 342: 118-123.

Werner, BT, Koch, A, Šečić, E, Engelhardt, J, Jelonek, L, Steinbrenner, J and Kogel, K-H 2021. *Fusarium graminearum* DICER-like-dependent sRNAs are required for the suppression of host immune genes and full virulence. *PLoS One* 16: e0252365.

Whisson, SC, Vetukuri, RR, Avrova, AO and Dixelius, C 2012. Can silencing of transposons contribute to variation in effector gene expression in *Phytophthora infestans*? *Mob. Genet. Elements* 2: 110-114.

Wightman, B, Ha, I and Ruvkun, G 1993. Posttranscriptional regulation of the heterochronic gene lin-14 by lin-4 mediates temporal pattern formation in *C.*

*elegans*. *Cell* 75: 855-862.

Xu, M, Guo, Y, Tian, R, Gao, C, Guo, F, Voegele, RT, Bao, J, Li, C, Jia, C and Feng, H 2020. Adaptive regulation of virulence genes by microRNA-like RNAs in *Valsa mali*. *New Phytol.* 227: 899-913.

Xu, M, Li, G, Guo, Y, Gao, Y, Zhu, L, Liu, Z, Tian, R, Gao, C, Han, P, Wang, N, Guo, F, Bao, J, Jia, C, Feng, H and Huang, L 2022. A fungal microRNA-like RNA subverts host immunity and facilitates pathogen infection by silencing two host receptor-like kinase genes. *New Phytol.*: 1.

Yan, Z, Hu, HY, Jiang, X, Maierhofer, V, Neb, E, He, L, Hu, Y, Hu, H, Li, N and Chen, W 2011. Widespread expression of piRNA-like molecules in somatic tissues. *Nucleic Acids Res.* 39: 6596-6607.

Yang, S, Dai, R, Salaipeth, L, Huang, L, Liu, J, Andika, IB and Sun, L 2021. Infection of two heterologous mycoviruses reduces the virulence of *Valsa mali*, a fungal agent of apple valsa canker disease. *Front. Microbiol*: 1092.

Ye, R, Chen, Z, Lian, B, Rowley, MJ, Xia, N, Chai, J, Li, Y, He, XJ, Wierzbicki, AT and Qi, Y 2016. A dicer-independent route for biogenesis of siRNAs that direct DNA methylation in *Arabidopsis*. *Mol. Cell* 61: 222-235.

Yin, C, Zhu, H, Jiang, Y, Shan, Y and Gong, L 2020. Silencing dicer-like genes reduces virulence and sRNA generation in *Penicillium italicum*, the cause of citrus blue mold. *Cells* 9: 363.

Yu, J, Lee, K-M, Cho, WK, Park, JY and Kim, K-H 2018. Differential contribution

of RNA interference components in response to distinct *Fusarium graminearum* virus infections. *J. Virol.* 92: e01756-01717.

Zamore, PD, Tuschl, T, Sharp, PA and Bartel, DP 2000. RNAi: double-stranded RNA directs the ATP-dependent cleavage of mRNA at 21 to 23 nucleotide intervals. *Cell* 101: 25-33.

Zanini, S, Šečić, E, Busche, T, Galli, M, Zheng, Y, Kalinowski, J and Kogel, K-H 2021. Comparative analysis of transcriptome and sRNAs expression patterns in the *Brachypodium distachyon—Magnaporthe oryzae* pathosystems. *Int. J. Mol. Sci.* 22: 650.

Zhang, B-S, Li, Y-C, Guo, H-S and Zhao, J-H 2022. *Verticillium dahliae* secretes small RNA to target host miR157d and retard plant floral transition during infection. *Front. Plant Sci.* 13.

Zhang, X, Segers, GC, Sun, Q, Deng, F and Nuss, DL 2008. Characterization of hypovirus-derived small RNAs generated in the chestnut blight fungus by an inducible DCL-2-dependent pathway. *J. Virol.* 82: 2613-2619.

Zhou, R and Rana, TM 2013. RNA-based mechanisms regulating host–virus interactions. *Immunol. Rev.* 253: 97-111.

Zhuo, Y, Gao, G, an Shi, J, Zhou, X and Wang, X 2013. miRNAs: biogenesis, origin and evolution, functions on virus-host interaction. *Cell. Physiol. Biochem* 32: 499-510.

# CHAPTER II

# Comparative profiling of canonical and non-canonical small RNAs in the rice blast fungus, *Magnaporthe oryzae*

This chapter was published in Frontiers in Microbiology

Lee, H. et al. (2022) *Front. Microbiol.* 3657.

# ABSTRACT

RNA interference (RNAi) is divided into canonical, Dicer-dependent and non-canonical, Dicer-independent pathways according to Dicer protein dependency. However, sRNAs processed in a Dicer-independent manner have not been reported in plant pathogenic fungi, including *Magnaporthe oryzae.* We comparatively profiled the Dicer-dependent and -independent sRNAs of *M. oryzae*. Dicer-dependent sRNAs were 19-24-nt in length, had low strand-specificity, and showed a preference for uracil at the 5'-end. By contrast, Dicer-independent sRNAs presented irregular patterns in length distribution, high strand-specificity, and a preference for cytosine at the penultimate position. Dicer-dependent sRNA loci were mainly associated with LTR-transposons, while Dicer-independent sRNAs were associated with protein-coding genes and transposons. We identified *MoERI*-1, a non-canonical RNAi component, and profiled the sRNA and mRNA transcriptomes of Δ*Moeri-1* at the mycelia and conidiation stages, as the mutant showed increased conidiation. We found that genes involved in conidiation and cell cycle were upregulated by *MoERI-1* deletion. Furthermore, a comparison between sRNA and mRNA transcriptome revealed that MoERI-1-dependent sRNAs mediate the regulation of gene expression. Overall, these results showed that *M. oryzae* has non-canonical RNAi pathways distinct to the Dicer-dependent manner and exploits MoERI-1-dependent sRNAs to regulate the conidiation process.

# INTRODUCTION

Small non-coding RNAs (sRNAs) are the core component of RNA interference (RNAi), mediating gene regulation at the post-transcriptional and transcriptional levels (Buhler and Moazed, 2007;Ghildiyal and Zamore, 2009). In the canonical RNAi pathway, a double-stranded RNA (dsRNA)-specific ribonuclease Dicer cleavages hairpin RNA or dsRNA into sRNAs. These sRNAs are loaded into Argonaute (AGO) protein to form RNA-induced gene silencing complex (RISC), which mediates the degradation of target RNAs or translational repression (Drinnenberg et al., 2009). sRNA species generated by canonical RNAi are generally categorized as siRNA and miRNA according to their sources and related RNAi components.

Since quelling, the first example of RNAi in fungi was reported in *Neurospora crassa*, canonical RNAi has been extensively studied in fungi as well as in animals and plants. Quelling and meiotic silencing of unpaired DNA (MSUD) are sRNA-based genome defense mechanisms reported in *N. crassa*. In *Schizosaccharomyces pombe*, heterochromatic siRNA (het-siRNA) processed by Dcr1 guides the RNA-induced transcriptional silencing (RITS) complex to the nascent target RNA. The guided RITS complex recruits chromatin modifying enzymes to methylate lysine 9 of histone 3, leading to heterochromatin formation (Billmyre et al., 2013). Exonic-siRNAs (ex-siRNA), which require Dicer enzymes for biogenesis, regulate the developmental processes in *Fusarium graminearum*, *Mucor circinelloides*, and *Trichoderma atroviride* (Carreras-Villasenor et al., 2013;Nicolas et al., 2010;Son et

al., 2017). Fungi with a number of transposons typically have defense systems to limit transposon and retrotransposon activity via quelling-like RNAi pathways, mediated by transposon-derived siRNAs (Torres-Martinez and Ruiz-Vazquez, 2017).

Non-canonical pathways in which Dicer proteins do not participate have been reported to be responsible for the biogenesis of specific sRNAs. Piwi-interacting RNAs (piRNAs), which silence transposons in germ line cells, require AGO proteins and their catalytic activity, instead of Dicers (Siomi et al., 2011). In *Arabidopsis*, siRNAs independent of DCLs (sidRNAs) interact with AGO4 and 3'-5' exonucleases trimming sidRNAs to the proper size, and were proposed to initiate the *de novo* DNA methylation of transposons (Ye et al., 2016). *S. pombe* also exploits a 3'-5' exonuclease, Triman, to generate primal small RNAs (priRNAs) that trigger the positive-feedback loop of siRNA generation and heterochromatin assembly (Marasovic et al., 2013). In *N. crassa*, Dicer-independent siRNAs (disiRNAs), derived from both strands of the genome, contribute to transcriptional silencing of target genes including *FRQ* (Lee et al., 2010). *NcERI-1* is responsible for the generation of disiRNAs derived from disiRNA loci where convergent transcriptions occur. Unlike ERI-1 of *Drosophila*, human, mouse and *S. pombe*, which binds to dsRNAs via the SAP domain, *NcERI-1* recognizes the 3' end G-rich motif of single strand RNAs via an RNA recognition motif (RRM) and zinc-finger domain (Dang et al., 2016;Thomas et al., 2014).

Advances in next-generation sequencing and bioinformatics have enabled massive profiling of sRNAs in fungi. sRNAs with roles in genome defense against viruses and transposable elements have been profiled in fungi (Nicolás and Ruiz-Vázquez,

2013;Torres-Martinez and Ruiz-Vazquez, 2017). Possible roles of sRNAs have also been suggested in responses to exogenous stimuli under various environmental conditions in *Aspergillus flavus* (responses to water activity and temperature) and *M. circinelloides* (resistance to antifungal drug) (Bai et al., 2015;Calo et al., 2017). Profiling of sRNAs during host-pathogen interactions has revealed that sRNAs function not only as endogenous regulators but also as effectors in *Botrytis cinerea*, *Verticillium dahliae*, and *Puccinia striiformis* (Wang et al., 2017;Weiberg et al., 2013).

*M. oryzae* is the causal agent of rice blast, which causes severe yield losses in cultivated rice worldwide. Due to the scientific achievements in both fungus and the host, and global economic importance, the interaction between *M. orzyae* and rice has been a model pathosystem for studies on molecular basis of pathogenesis (Dean et al., 2012). *M. oryzae* has two Dicer-like proteins (MoDCL1 and MoDCL2), three AGO proteins (MoAGO1, MoAGO2 and MoAGO3), and three RNA-dependent RNA polymerases (MoRdRP1, MoRdRP2, and MoRdRP3). MoDCL2 plays main role in hairpin-RNA-induced gene silencing, while MoDCL1 rarely contributes to siRNA production from hairpin RNA (Kadotani et al., 2004;Kadotani et al., 2008). *M. oryzae* sRNAs have diverse genomic origins and dynamically changed according to the appressorium development, diverse stresses and during rice infection (Nunes et al., 2011;Raman et al., 2013). Profiling of sRNAs from RNAi mutants showed that MoDCL2, MoRdRP2, and MoAGO3 are responsible for sRNA production and transcript regulation, particularly from transposons and intergenic regions (Raman et al., 2017). Sequencing of Ago-binding sRNA libraries suggested that MoAGO3 is

the major AGO protein in RNA silencing of transposons and viral RNAs (Nguyen et al., 2018). However, non-canonical sRNAs have not been studied in *M. oryzae* or in other plant pathogenic fungi.

In this study, we comparatively profiled canonical and non-canonical sRNAs by sequencing sRNA libraries from the wild-type (WT), DCLs mutants. We showed that Dicer-dependent sRNAs share features with canonical sRNAs, whereas Dicer-independent sRNAs have distinct characteristics, suggesting non-canonical RNAi mechanisms in *M. oryzae*. We also identified a non-canonical RNAi component, MoERI-1. MoERI-1-dependent sRNAs may be involved in vegetative growth and conidiation of *M. oryzae*.

# MATERIALS AND METHODS

## I. Generation of targeted-gene deletion mutant and complementation

*M. oryzae* KJ201 (wild type) was obtained from the Center for Fungal Genetic Resources (CFGR) at Seoul National University, Seoul, Korea. To produce targeted gene deletion construct, the upstream and downstream flanking regions of RNAi-associated genes (*MoDCL1*, *MoDCL2* and *MoERI*-1) were amplified from the genomic DNA (gDNA) of the wild type. The hygromycin B phosphotransferase gene (HPH) cassette and the geneticin resistance cassette were amplified from pBCATPH and pII99, respectively (Kim et al., 2005;Lee et al., 2003). Constructs for targeted-gene deletion were produced by double-joint PCR using upstream flanking, downstream flanking, and hygromycin/geneticin-resistance cassette. Transformation and selection of mutants were performed as previously described (Lim and Lee, 2020). To generate the double gene deletion mutant of *MoDCL1* and *MoDCL2*, MoDCL2 was replaced with HPH construct first, and the geneticin-resistance construct were introduced into Δ*Modcl2* protoplasts. For complementation of *MoERI-1*, constructs containing ORF and promoter were amplified from the gDNA of the wild type and inserted into Δ*Moeri-1* protoplasts with geneticin cassette. The complemented strain was selected on TB3 agar with 800 ppm of geneticin, and selected by PCR using the ORF primers. All strains used in this research were deposited in the CFGR (http://genebank.snu.ac.kr).

## II. Extraction and sequencing of sRNA and mRNA

To prepare total mycelial RNA, fungal mycelia were incubated in liquid complete medium (CM) at 25 °C for 4 days and collected for total mycelial RNA extraction. For preparation of total RNA from conidiation stage, conidiating mycelia were harvested as previously described (Park et al., 2013). Briefly, fungal mycelia incubated in CM at 25 °C for 4 days were collected and placed on sterile membrane filter (Whatman, Maidstone, England) laid on V8 agar medium. After 6 days of incubation sealed with parafilm, followed by one day unsealed incubation for aeration, the membrane filter with conidiation stage were collected and subjected to RNA extraction. Total RNA including sRNA was isolated using miRNeasy mini kit (Qiagen, Hilden, Germany) according to manufacturer's instructions. The quality and concentration of each sample were checked by Agilent 2100 Bioanalyzer or 2200 TapeStation (Agilent Technologies, CA, USA). Three mycelia samples of each strain were independently used for RNA extraction, and the RNA samples were pooled for the synthesis of one cDNA library. Three independent cDNA libraries for the WT and two for mutant strains were constructed (KJL1-3, D1L1-2, D2L1-2, and D12L1-2). Construction of cDNA libraries of sRNA samples and their sequencing were performed at Macrogen (Seoul, Korea). cDNA libraries of sRNAs were constructed from total RNA samples using TruSeq Small RNA Library Prep Kit (Illumina, CA, USA) and sequenced by Illumina Hiseq2500. cDNA library construction and sequencing of mRNA were performed at National Instrumentation Center for Environmental Management at Seoul National University (NICEM, Seoul, Korea). cDNA libraries were constructed using TruSeq RNA Sample Prep Kit (Illumina) and

paired-end sequencing of each sample was conducted by Illumina HiSeq2500

## III. sRNA and mRNA data analysis

As the first step of raw sRNA read processing, adaptor sequences were removed by Cutadapt v1.8.1 (Martin, 2021). Reads were filtered by quality and size using Sickle v1.33 (Joshi and Fass, 2011). Reads ranging 18 – 30-nt with at least two copies in each library were used for genome mapping to reduce the possible sequencing error and degradation products. Processed reads were mapped to the reference genome of the *M. oryzae* strain 70-15 (MG8) from National Center for Biotechnology Information (NCBI, https://www.ncbi.nlm.nih.gov/) using bowtie v1.2.2 (Langmead et al., 2009). Read abundance was counted by the number of copies and multiple-mapped reads were weighted by ShortStack3 with 'U' method (Johnson et al., 2016). Distinct genome-matched reads were calculated based on the hits. To compare the different libraries by fixing the coordinate, sRNA loci were clustered by ShortStack3. The abundance of each loci was normalized to reads per kilobase per million reads (RPKM). sRNA loci with following conditions were used for further analyses: distinct read > 5, combined read abundance of loci > 10 RPKM, length of loci > 100 bp. sRNA loci ≥ 4-fold differences in mutant libraries compared to the WT libraries were referred to as "Dicer or MoERI-1 dependent loci" in this study. Dicer-independent sRNA loci were determined as sRNA loci excluding the loci with more than 2-fold decrease in mutant libraries compared to the WT libraries.

Raw mRNA reads were processed to remove low-quality reads and trim adapter sequences using NGS QC Toolkit v2.3.3 (Patel and Jain, 2012). The resulting reads

were mapped against the *M. oryzae* reference genome (MG8) using HISAT2 v2.0.4 (Kim et al., 2019). The transcriptome was assembled using the genome-guided method of StringTie v1.3.3 (Pertea et al., 2015). We used fragments per kilobase of transcript per million mapped read pairs (FPKM) as the expression value.

## IV. Mycelial growth, conidiation, conidial germination and appressorium formation

All strains were cultured in modified complete agar medium (CMA) and minimal agar medium (MMA) at 25°C for 9 days for assessment of mycelial growth and colony morphology. Conidia were collected from cultures on V8 agar after incubation for 7 or 11 days. For aeration, plates were unsealed for 24 hours on the last day of incubation. Conidiation was measured under a microscope using a hemacytometer. To assess conidial germination and appressorium formation, 50 μL of conidial suspensions (2 x $10^4$/mL) was dropped on a hydrophobic cover glass at 25°C. Conidial germination and appressorium formation were evaluated under a microscope after incubation for 2 and 8 hours, respectively. Conidiogenesis was observed as described previously (Goh et al., 2011;Lau and Hamer, 1998). Hyphae from conidia were incubated with Calcofluor white (CFW, 10 μg/mL, Sigma Aldrich, USA) at 25°C for 5 min to stain septa, and visualized using a fluorescence microscope (Carl Zeiss, Oberkochen, Germany).

## V. Pathogenicity test

Pathogenicity tests were performed using the susceptible rice cultivar, Nakdongbyeo (*Oryzae sativa*) as previously described (Lim et al., 2018). Briefly, to perform spray inoculation assay, 10 mL of conidia suspension ($5 \times 10^4$ /mL, supplemented with 250 ppm of Tween 20) was inoculated on 4-week-old rice seedlings. Inoculated rice plants were incubated in humid and dark chamber at 25 ◦C for 1 day (100% relative humidity) and then incubated in growth chamber at 28 ◦C for 5 days. For performing sheath inoculation assay, conidia suspension ($2 \times 10^4$ /mL) was inoculated into the sheath of 6-week-old of rice. Inoculated rice sheath was incubated at 25 ◦C for 48 h in a humid chamber. After then, invasive hyphal growth was observed under a microscope.

# RESULTS

## I. Profiling of canonical sRNAs in *M. oryzae*

To profile *M. oryzae* sRNAs in the canonical RNAi pathway, two single deletion mutants (Δ*Modcl1* and Δ*Modcl2*) and one double deletion mutant (Δ*Modcl1/2*) were generated (Figure 1). From mycelia of the WT strain KJ201 and the deletion mutants, size-fractionated small RNAs were isolated and used for cDNA library construction and sequencing (Table 2). Sequencing of two KJ201 libraries (KJL1 and KJL2) revealed discrete patterns, mostly due to altered sRNA lengths (Figure 2A, B). Although the length distribution of KJL1 reads peaked at 20-nt, KJL2 showed a major peak at 23-nt and minor peak at 20-nt. To assess repeatability, we performed additional experiment of KJ201 sequencing. The sequencing result of KJL3 was similar to that of KJL2 (Figure 2A, B). Distinct reads shared by replicates accounted for > 89% of the total reads, implying that the different length distribution of KJL1 was caused by a change in the abundance of the common distinct reads (Figure 2D, E). Pearson correlation analysis based on the read abundance of sRNA-producing loci showed that the read abundances of sRNA-producing loci between KJ201 replicates are highly correlated (Figure 2C). Although the majority of sRNA-producing loci were maintained through replicates, we selected the sequencing results of the library set in second experiments (KJL2, D1L2, D2L2 and D12L2) for further analyses. After adaptor removal and quality filtering, reads of 18-30-nt were mapped to the *M. oryzae* reference genome, resulting in 2-8 million genome mapped reads. By comparing sRNA reads among the four libraries, reads in KJ201 and

Δ*Modcl1*, but not Δ*Modcl2* and Δ*Modcl1/2*, which are highly likely to be generated by MoDCL2, accounted for the largest portion (17.9%) of whole distinct reads, and the second-largest portion (19.2%) of whole total reads (Figure 3A, B). Reads detected in all four libraries might include the both types of reads produced in Dicer-dependent and -independent manner. Such common reads accounted for only 9.1% of distinct reads, but the largest portion (61.7%) of total reads. We next investigated the genomic origin, length distribution and 5'-end frequencies of the sRNAs. The mapped reads from *M. oryzae* WT mainly originated from the repeat region (79.4%) in which there were almost equal amounts of sRNAs from sense and antisense strands (Figure 4A). The nucleotides at the 5'-ends were highly biased toward uracil (47.9%) and most reads were 19-24-nt in length (88% of total reads), with a peak at 23-nt (Figure 4B, C). The genomic origin proportions, length distributions and 5'-end frequencies of Δ*Modcl1* were similar to those of the WT. Comparison of KJ201 and Δ*Modcl1* showed that the common reads accounted for 94.9% of total reads and mainly affected the sRNA features of each library (Figure 5A-C). In *MoDCL2*-deleted mutants (Δ*Modcl2* and Δ*Modcl1/2*), the proportions of sRNAs from the antisense strand of repeats were decreased, and those from the sense strands of exons were increased compared to the WT (Figure 4A). In addition, those biases towards certain size classes (19-24-nt) and 5'-end uracil in the wild type were abolished by the deletion of *MoDCL2* (Figure 4B, C). In a comparison of reads against KJ201, ~20% of distinct reads and ~70% of total reads were shared (Figure 6A). This proportion of common reads between KJ201 and Δ*Modcl1/2* was smaller than that between KJ201 and Δ*Modcl1* (Figure 5A, 6A). Unlike the *MoDCL2*-deleted mutant

libraries, the KJ201 library-specific reads accounted for large proportions of both distinct reads and total reads possibly because of the Dicer-dependent sRNAs. Common reads between KJ201 and Δ*Modcl1/2* were mainly derived from the repeat region with sense orientation (Figure 6B, C). Intriguingly, the proportions of 5'-U reads of each size peaked at 19-20-nt not only in the WT and Δ*Modcl1* but also in Δ*Modcl2* and Δ*Modcl1/2* (Figure 4D, 7C).

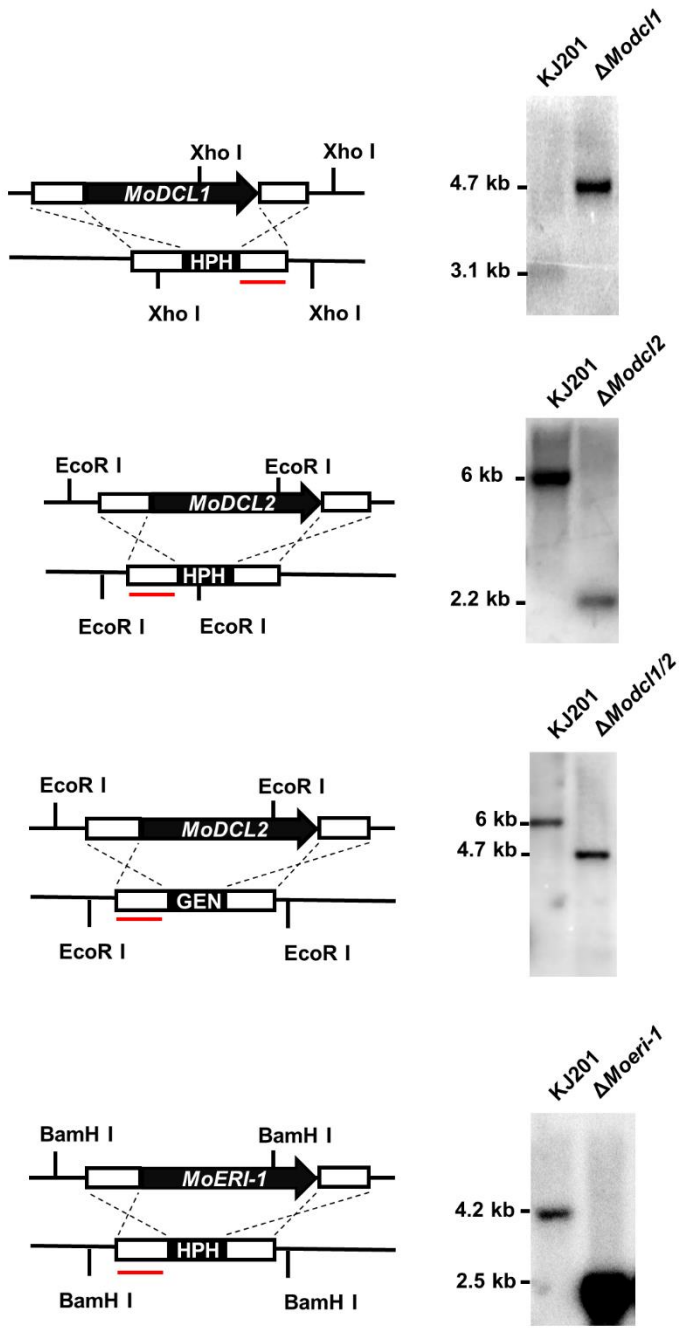


**Figure 1. Confirmation of target gene deletion by Southern blotting.** Genomic DNAs of KJ201 (WT) and deletion mutants were isolated and digested with Xho I,

EcoR I, or BamH I. The upstream or downstream construct of each gene was used as a probe for Southern blot analysis. Red bar indicates the location of the probe used in each experiment. Primers used in the experiments are listed in Table 2.

**Table 1. Primers used in this study**

| Name | Primers |
|---|---|
| MoDCL1_5'F | ACTGGTCGCGCATACTCCTC |
| MoDCL1_L+5'R | cctccactagctccagccaagccGCGTACTTGGCACATTTCCTGC |
| MoDCL1_L+3'F | gttggtgtcgatgtcagctccggagGGCTAGGGTAGAGCCCATATACAC |
| MoDCL1_3'R | CCACGCAGATGTGAAGATGACCTC |
| MoDCL1_5'NF | CTCCGAGACCTGCTCTTTAGTGC |
| MoDCL1_3'NR | GTCCTTGATCCCCACATGGTCC |
| MoDCL2_5'F | GAGATGAATGGCGACTCCATCGAG |
| MoDCL2_L+5'R | cctccactagctccagccaagccGGTAGCAGAGTGGGCGGTAATG |
| MoDCL2_L+3'F | gttggtgtcgatgtcagctccggagAAGGAGAAACCGCGGCCTAC |
| MoDCL2_3'R | CACTGATGACAGGACTCCCTGAG |
| MoDCL2_5'NF | TCGCACAGGGAGGTTAGCTTG |
| MoDCL2_3'NR | CAAGGGTATCTGCTGCCGTCTG |
| MoERI-1_5'F | AAAGCAACCTCACACCGCATGTC |
| MoERI-1_L+5'R | cctccactagctccagccaagccGGCAAGAAGCCGAACAGTGGA |
| MoERI-1_L+3'F | gttggtgtcgatgtcagctccggagAAGTCGCCCGCGTAAGATCAACA |
| MoERI-1_3'R | TGCTCATGACGCTCCAGGTCATAC |
| MoERI-1_5'NF | CCACGCGAAGATGTCAGTGTCA |
| MoERI-1_3'NR | CGGGGATCAGTGACGAACAACTCA |

*Letters in lower case indicate HPH linker sequence.

**Table 2. Statistical summary of mycelial sRNA sequencing and processing**

| | **KJ201** | | **Δ*Modcl1*** | | **Δ*Modcl2*** | | **Δ*Modcl1/2*** | | **Δ*Moeri-1*** | |
|---|---|---|---|---|---|---|---|---|---|---|
| | Redundant | Distinct | Redundant | Distinct | Redundant | Distinct | Redundant | Distinct | Redundant | Distinct |
| Size & quality filtered-reads | 25,513,775 | 2,373,285 | 26,651,112 | 2,427,881 | 21,819,728 | 1,462,440 | 15,456,677 | 1,116,322 | 17,908,050 | 1,855,090 |
| Reads ≥ 2 | 24,001,969 | 861,479 | 25,074,785 | 851,554 | 20,851,803 | 494,515 | 14,692,959 | 352,604 | 16,736,831 | 683,871 |
| Genome-mapped reads | 8,077,611 | 339,877 | 7,490,250 | 336,729 | 3,069,056 | 240,685 | 1,968,901 | 160,826 | 5,959,877 | 280,201 |
| Nonstructural reads | 7,550,911 | 325,225 | 6,834,360 | 321,466 | 2,266,710 | 223,004 | 1,426,058 | 146,435 | 5,636,951 | 268,493 |

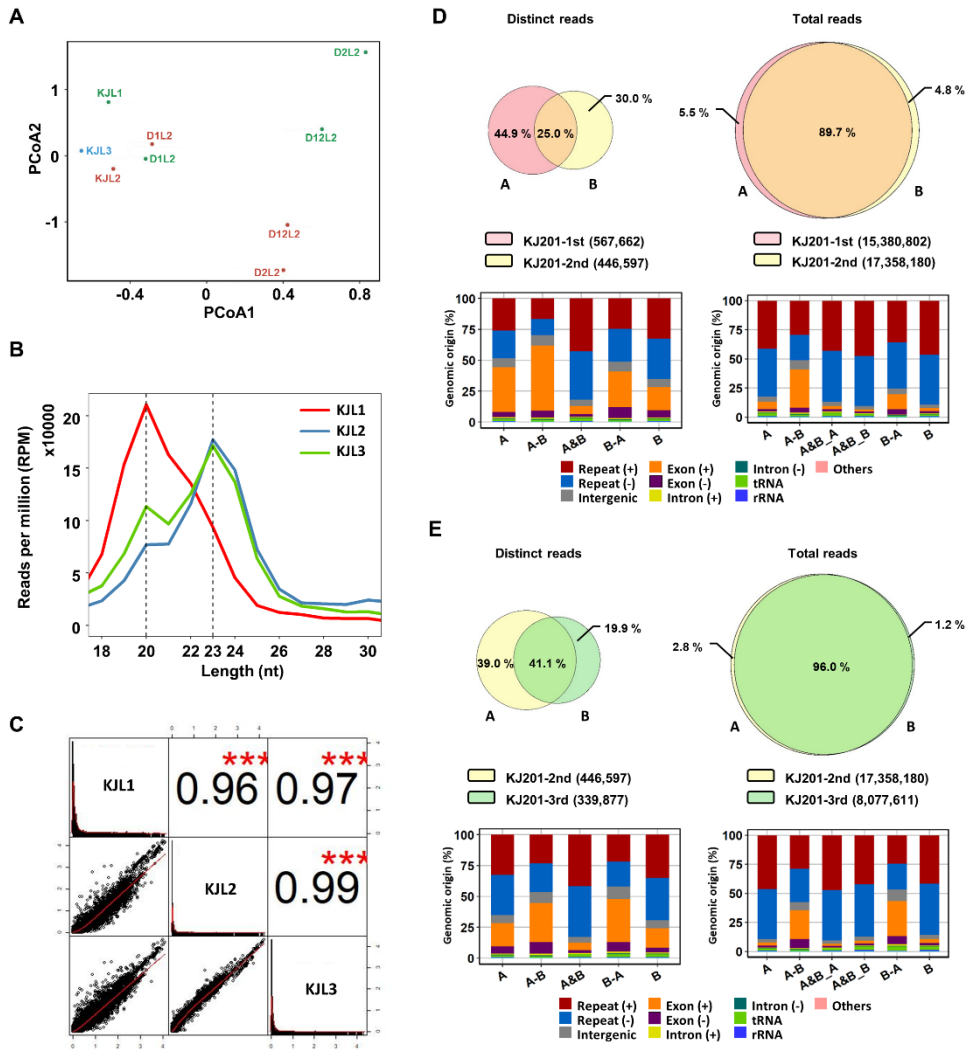


**Figure 2. Repeatability of sRNA seq data**. (A) Principal coordinates (PCoA) plot of sRNA seq libraries. (B) Length distributions of the KJ201 WT sRNA seq libraries. (C) Pearson correlation coefficients between the WT libraries based on sRNA loci. *** $p < 0.001$. (D)Venn diagram of reads of KJ201-first and KJ201-second among distinct and total reads. (E) Venn diagram of reads of KJ201-second and KJ201-third among distinct and total reads. (D and E) Genomic origins are shown in the lower panel. “A” and “B” indicate the two libraries in the Venn diagram, “A-B” and “B-A’

are the differences between two sets, and “A&B” indicates the intersection of two libraries. Because the distinct reads of “A&B” can have different total read numbers in each library, the intersection was divided into “A&B_A” and “A&B_B” to compare the genomic origins of total reads.

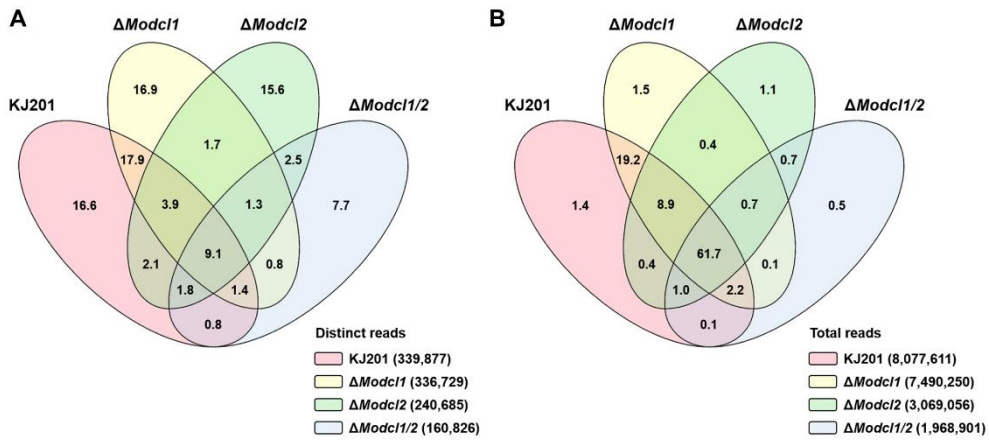


**Figure 3. Venn diagram of sRNAs profiled in the WT and *MoDCL* mutant libraries.** Venn diagram showing the proportions of distinct reads **(A)** and total reads **(B)** in the four libraries. Numbers in each section are percentages of read numbers relative to the sum of distinct reads or total reads from the four libraries.

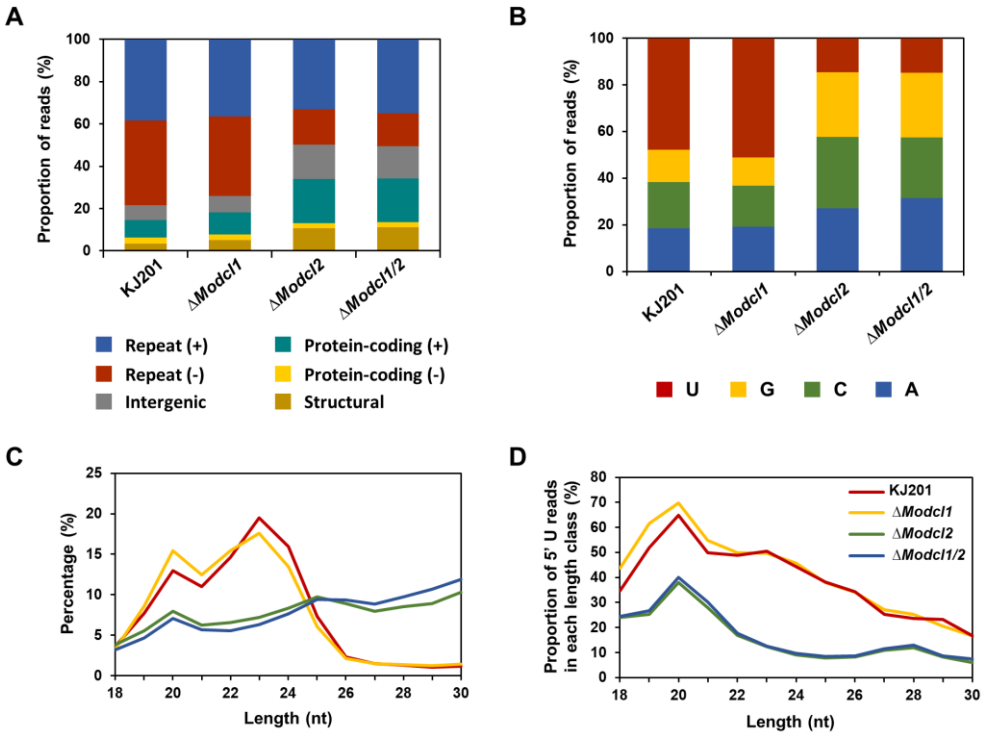


**Figure 4. Characteristics of *M. oryzae* sRNAs. (A)** Genomic origins of sRNAs. (+) and (-), sense strand and antisense strands, respectively. **(B)** Nucleotide composition at the 5'-ends of sRNAs. **(C)** Length distribution of sRNAs. **(D)** Proportions of 5'-uracil reads in each length class.

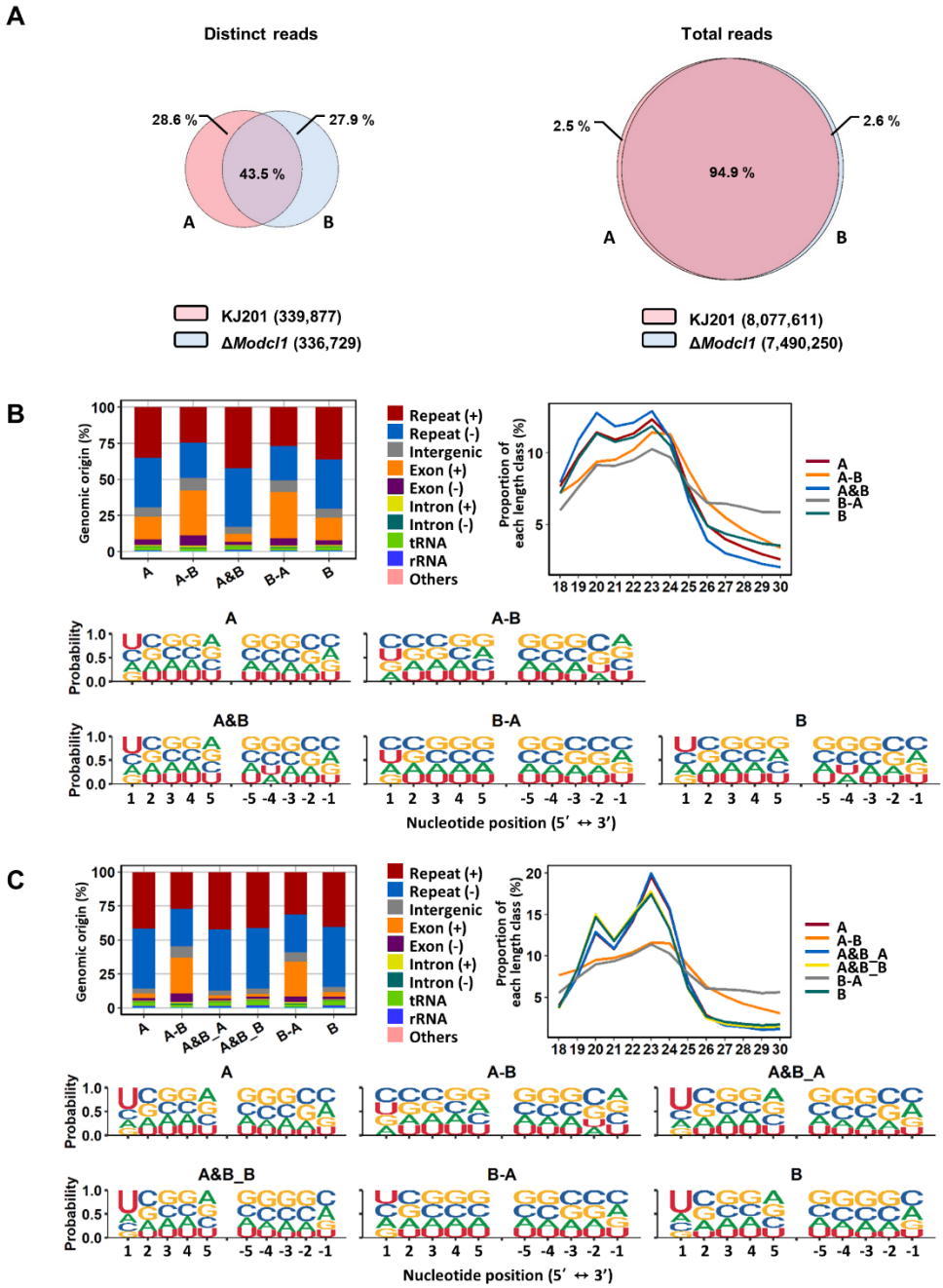


**Figure 5. Venn diagram of KJ201 and Δ*Modcl1* libraries using distinct and total sRNAs. (A)** Venn diagram showing the proportions of distinct and total reads from KJ201 and Δ*Modcl1*. Genomic origin, length distribution, and nucleotide

composition were investigated using the distinct reads **(B)** and total reads **(C).**

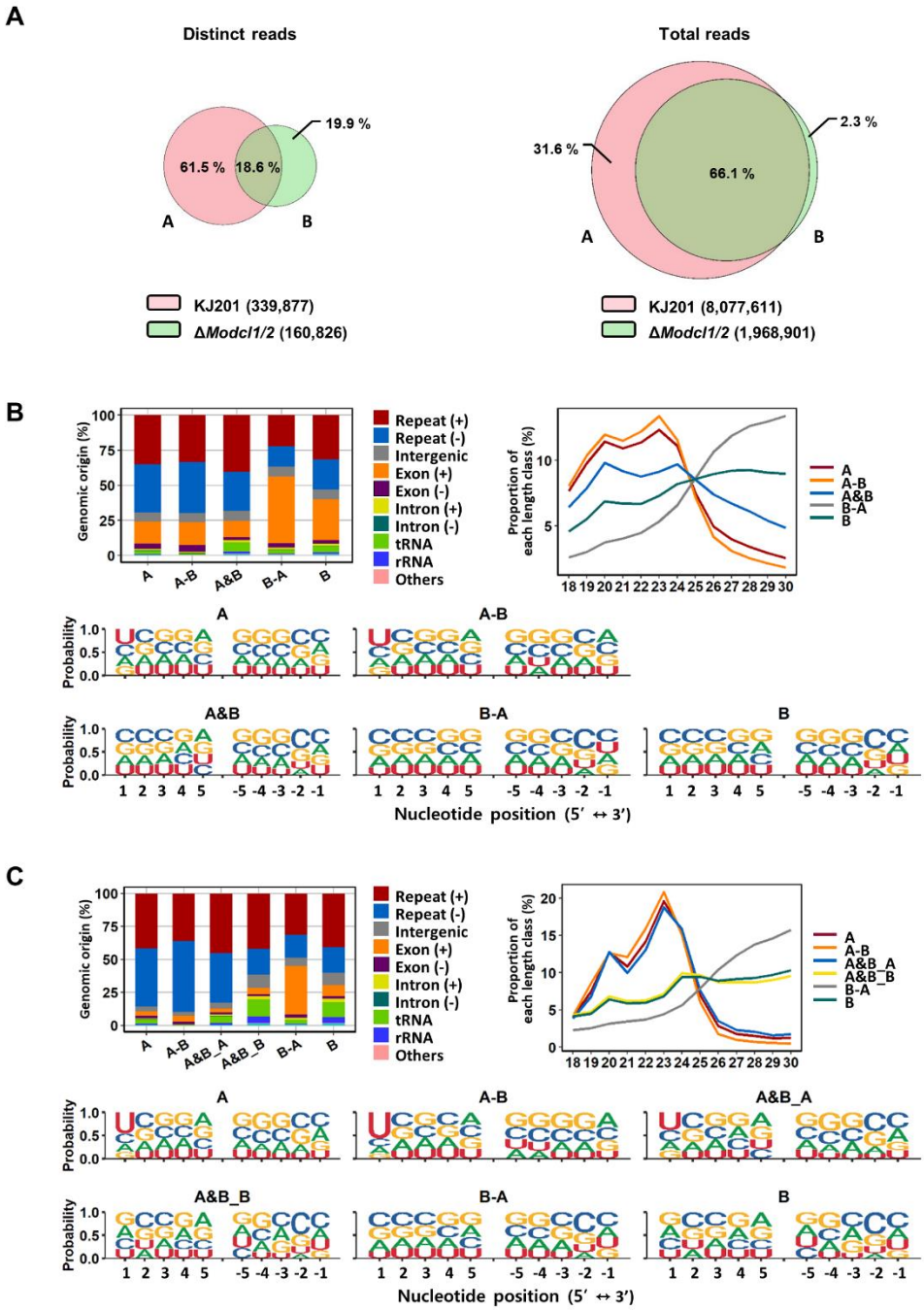


**Figure 6. Venn diagram of KJ201 and Δ*Modcl1/2* libraries using distinct and total sRNAs. (A)** Venn diagram of the proportions of distinct and total reads from

KJ201 and Δ*Modcl1/2.* Genomic origin, length distribution, and nucleotide composition were investigated using the distinct reads **(B)** and total reads **(C)**.

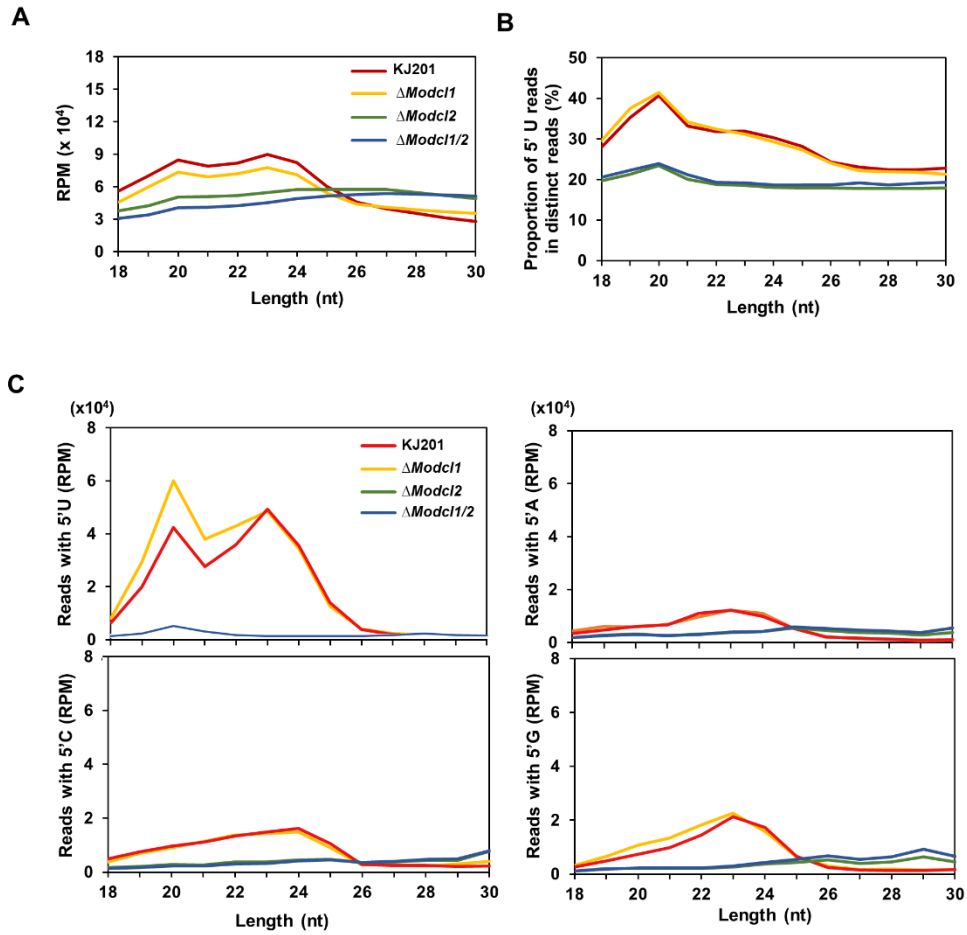


**Figure 7. Length distributions of sRNAs. (A)** Length distribution of distinct reads. **(B)** Proportions of reads with uracil at the 5'-end among the distinct reads. **(C)** Distribution of total reads according to 5'-end nucleotide.

## II. Identification of sRNA-producing loci

sRNA-producing loci were clustered with genome-aligned reads by ShortStack3. Among 6974 clustered loci, 939 were determined as sRNA-producing loci by following criteria: length ≥ 100-nt, number of distinct reads ≥ 5, and sum of read number from a locus ≥ 10 reads per kilobase per million (RPKM). Dicer-dependent sRNA-producing loci were defined as sRNA-producing loci with 4-fold decrease in normalized reads in Dicer-deleted mutants compared to the WT. Deletion of *MoDCL1* and *MoDCL2*, and double deletion of Dicer-coding genes decreased sRNA reads abundance in 94, 354 and 335 loci, respectively (Figure 8). Most of MoDCL1-dependent sRNA-producing loci overlapped with genes (95%; 89 out of 94), compared to 18% and 21% of MoDCL2- and MoDCL1/2-dependent sRNA loci, respectively (Table 3). Only 22 MoDCL1-dependent sRNA loci were overlapped with repeat elements, 20 of which were simple repeats. Additionally, 87% and 84% of MoDCL2- and MoDCL1/2-dependent sRNA loci overlapped with repeat elements, and most sRNA loci-associated repeat elements were LTR-retrotransposons. In a comparative analysis of canonical and non-canonical sRNAs, 335 loci that showed 4-fold decrease in Δ*Modcl1/2* were selected as Dicer-dependent sRNA loci, and 438 loci that showed no significant decrease in Δ*Modcl1/2* were determined as Dicer-independent sRNA loci (Table 3). Among Dicer-independent sRNA loci, most (67%) of them were associated with genes, followed by transposons, simple repeats and intergenic regions. Among Dicer-dependent sRNA loci-related repeat elements, an LTR-retrotransposon, GYMAG was the most frequent (41%), followed by the non-LTR type, MGR 583 (21%) (Figure 9A). By contrast, GYMAG accounted for 40%

of repeat elements associated with Dicer-independent sRNA loci, followed by simple repeats (21%) and MGR583 (9%) (Figure 9B). More than half of the gene-associated Dicer-dependent loci were also associated with repeat elements. Therefore, we hypothesized that genes associated with Dicer-dependent loci were located at genome regions with low gene density. As expected, genes associated with Dicer-dependent loci were more distant from neighboring genes than the average of protein-coding genes (Figure 9C). In the theory of two speed genome evolution, repeat rich regions are gene sparse, resulting much longer flanking distance between two genes (Dong et al., 2015). However, genes associated with Dicer-independent sRNA loci showed shorter-than-average flanking distances (Figure 9D). sRNAs from Dicer-dependent sRNA-producing loci were predominantly 19 – 24-nt range in WT and were irregularly distributed in 18 – 30-nt when *MoDCL1/2* were deleted (Figure 10A). However, sRNAs from Dicer-independent sRNA loci showed erratic length distribution patterns with or without Dicer proteins (Figure 10B). Compared to Dicer-dependent sRNA loci, Dicer-independent loci showed higher strand-specificity, indicating a greater likelihood of generating sRNAs from given strand (Figure 10C). sRNAs from Dicer-dependent loci showed uracil preference at the 5' end mainly due to 19-24-nt sRNAs, whereas sRNAs from Dicer-independent loci presented biased nucleotide composition with cytosine at the penultimate position, which was mainly observed in 25-30-nt sRNAs (Figure 10D, 11).

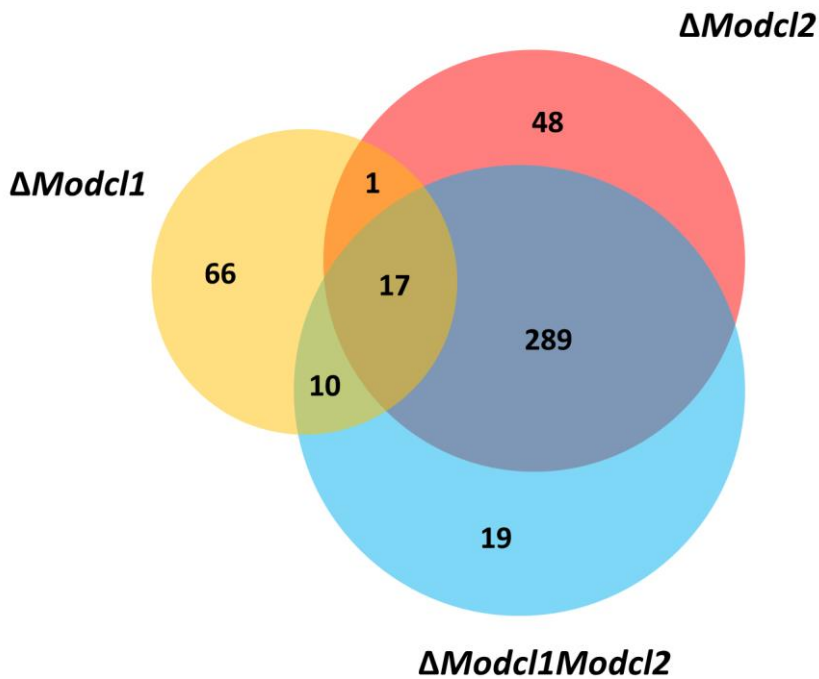


**Figure 8. Venn diagram of sRNA loci with reduced sRNAs in the dicer mutants.**

**Table 3. Number of sRNA-producing loci according to Dicer-dependency**

| Dependency | Total | Gene | Intergenic | LTR-retrostransposon | Non-LTR retrotransposon | DNA transposon | Simple repeat |
|---|---|---|---|---|---|---|---|
| MoDCL1 | 94 | 89 | 8 | 2 | 0 | 0 | 20 |
| MoDCL2 | 354 | 64 | 16 | 208 | 88 | 8 | 16 |
| MoDCL1/2 | 335 | 72 | 15 | 190 | 73 | 9 | 18 |
| Dicer-independent | 438 | 294 | 89 | 134 | 28 | 4 | 65 |
| MoERI-1 | 109 | 99 | 10 | 1 | 0 | 0 | 21 |

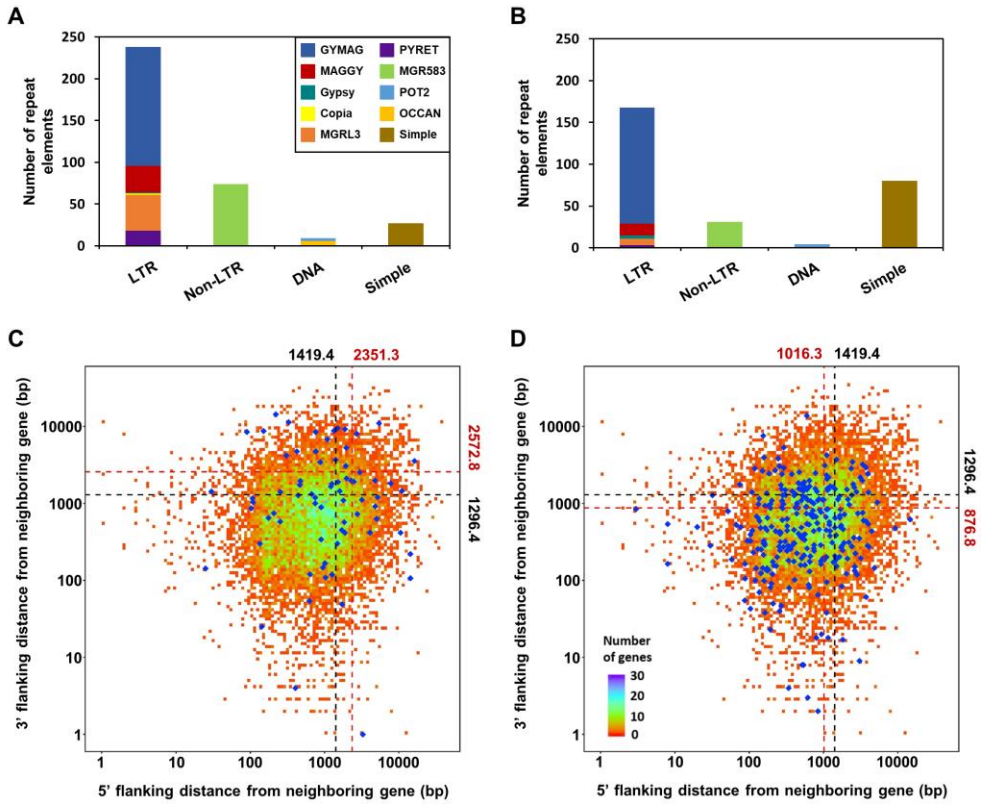


**Figure 9. Relationship between sRNA loci and repeat elements. (A)** Repeat elements associated with sRNA loci according to Dicer dependency. **(B)** Nearest-neighbor gene distance density plot for genes associated with sRNA loci according to Dicer dependency. Total protein-coding genes are plotted as the background; blue diamonds, genes associated with sRNA loci. Average distances are shown above and on the right, and are plotted as dotted lines. Black and red, total protein-coding genes and genes with sRNA loci, respectively.

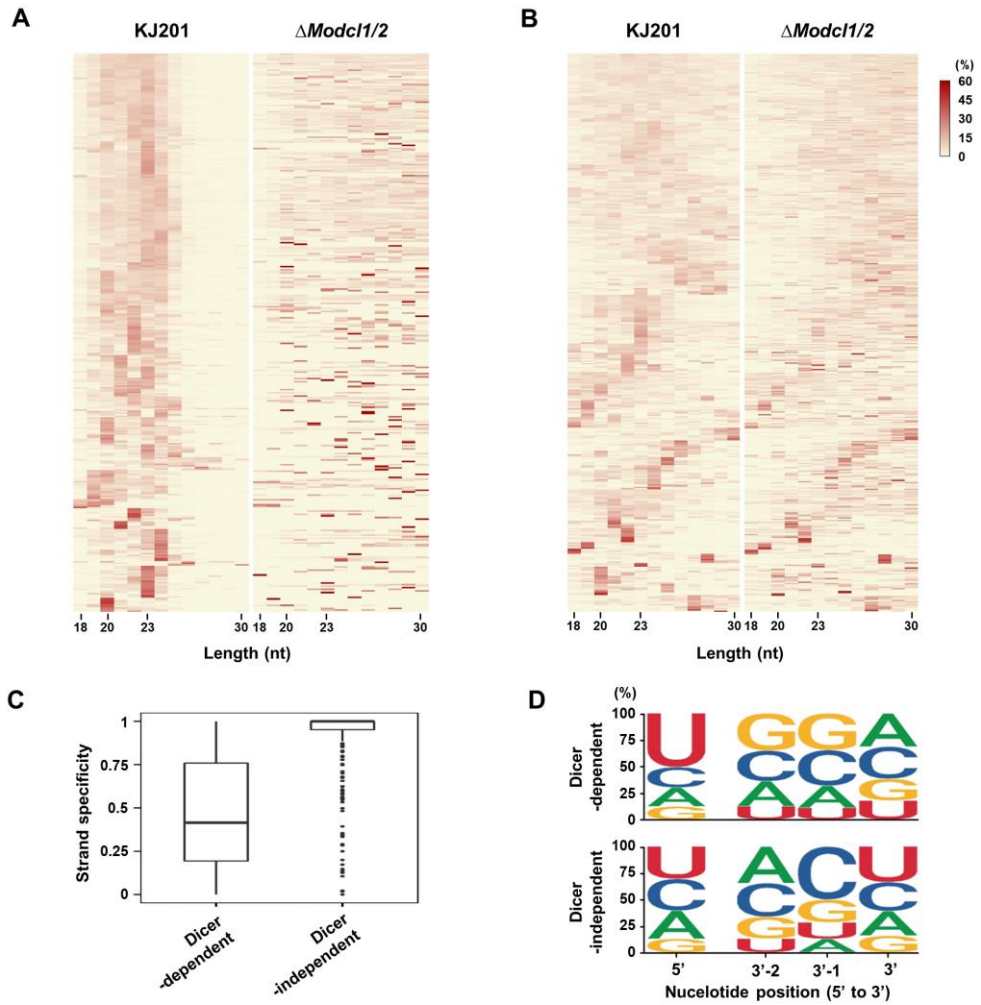


**Figure 10. sRNA features according to Dicer dependency.** Size distributions of sRNAs from **(A)** Dicer-dependent sRNA loci and **(B)** Dicer-independent sRNA loci as heatmaps. **(C)** Strand-specificity of sRNAs from sRNA-producing loci. **(D)** Probability of nucleotide composition at the 5'-end position and three positions from the 3'-end, using sRNAs from Dicer-dependent and -independent sRNA loci. Nucleotide composition analysis at whole positions is shown in Supplementary Figure 11.

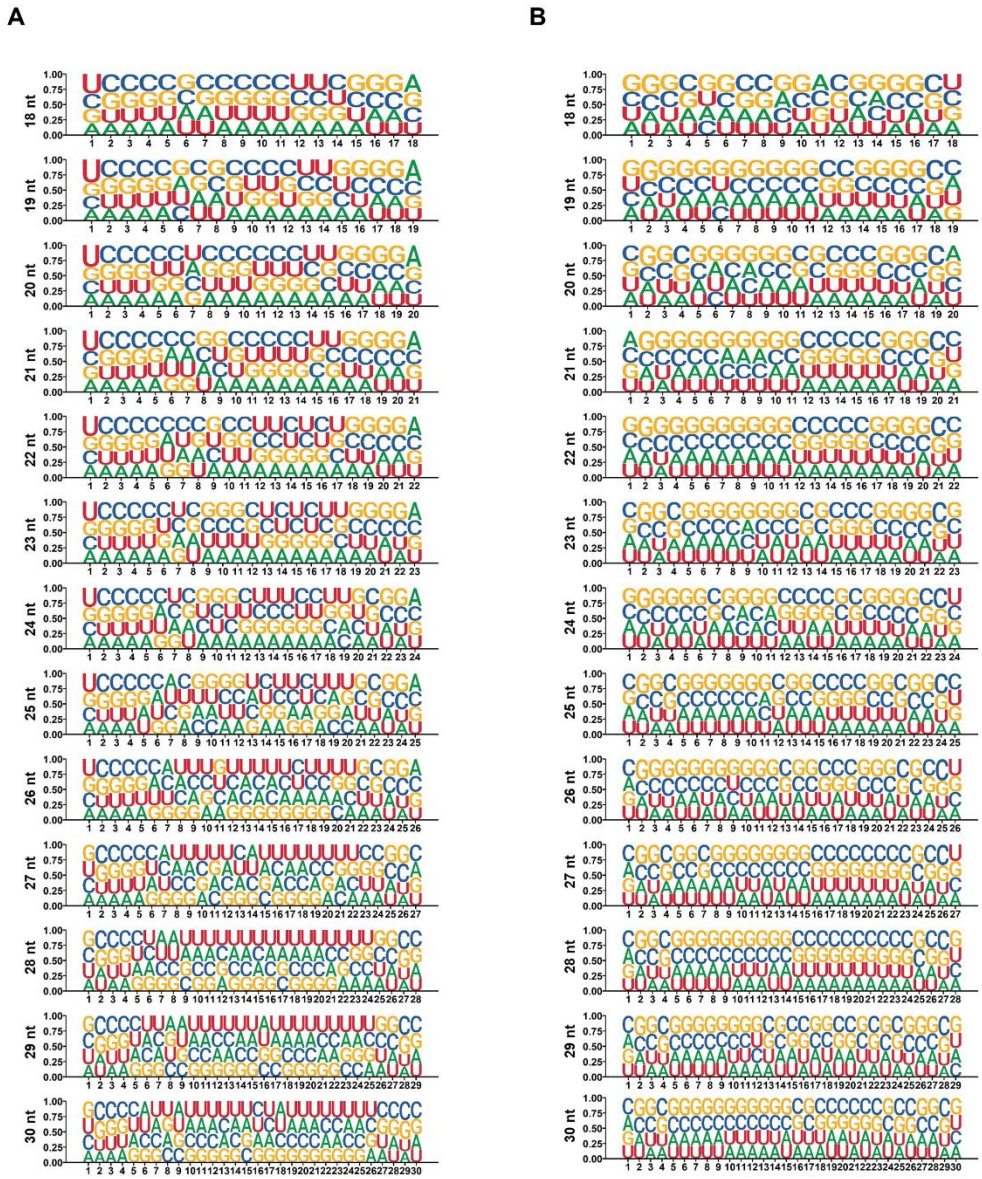


**Figure 11. Nucleotide compositions according to positions.** sRNAs from **(A)** Dicer-dependent and **(B)** Dicer-independent sRNA loci. *x*-Axis, nucleotide positions on sRNAs from 5' to 3'.

## III. Identification of MoERI-1, a non-canonical RNAi component

In non-canonical RNAi pathways, the central roles of Dicer and Ago are substituted by other exonucleases and Ago-like proteins. To identify the substitutes of the core RNAi component, Dicer, in non-canonical RNAi pathway, BLAST analyses of the previously reported non-canonical RNAses were performed. A well-conserved exonuclease, ERI-1, which was reported in *N. crassa*, showed high homology (100% coverage, 83.7% identity) with the protein coded by *MGG_07327*, therefore, *MGG_07327* was designated as *MoERI-1* (Figure 12). ERI-1 of *N. crassa* is responsible for the production of disiRNA, a non-canonical sRNA class of 22-nt major length and a 5'-end uracil bias, similar to QDE-2-binding sRNAs (Dang et al., 2016;Lee et al., 2010). Based on the high homology between two proteins, we hypothesized that MoERI-1 might have roles in Dicer-independent sRNA pathway in *M. oryzae*.

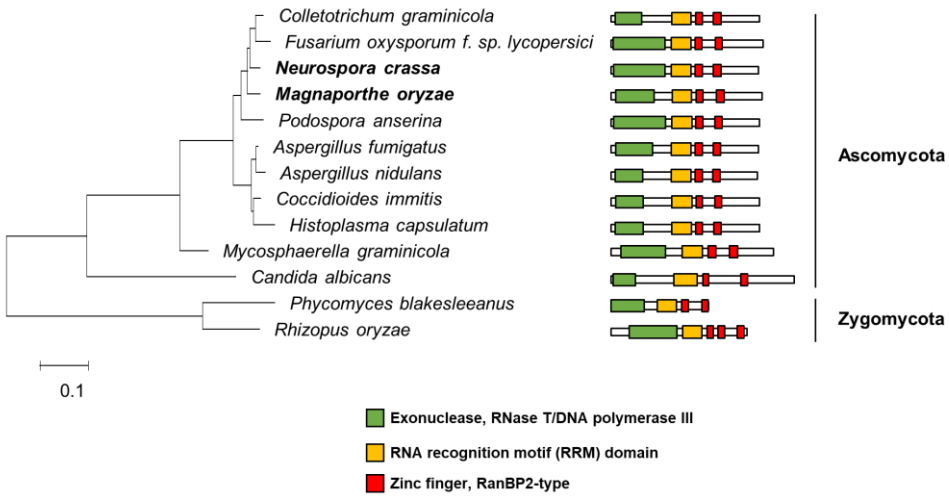


**Figure 12. Phylogenetic analysis of fungal ERI-1 proteins.** Neighbor-joining was performed by alignment of the exonuclease, RRM, and zinc-finger domains of *ERI-1* homologues confirmed by BLAST MASTRIX (CFGP; http://cfgp.riceblast.snu.ac.kr) using Goldstandard 3.0.

## IV. Deletion of *MoERI-1* reduced growth rate, increased conidiation, and caused abnormal septum formation

We generated a gene deletion mutant by the homologous recombination (Figure 1) and performed phenotypic analyses. Irrespective of aeration and incubation duration, Δ*Moeri-1* showed increased conidiation compared to the WT (Figure 13A). Additionally, the conidiophores carrying first conidia were observed earlier in Δ*Moeri-1* than the WT and Δ*Moeri-1* conidiophores had more conidia than the WT at the same time points (Figure 13B). Deletion of *MoERI-1* decreased the size of conidia and increased the proportion of conidia with one septum (Figure 13C). Such abnormal septum formation also observed in mycelia of Δ*Moeri-1*, with shorter distance between neighboring two septa (Figure 13D). Δ*Moeri-1* also showed decreased mycelial growth rate compared to the WT (Figure 13E). Altered phenotypes were restored in the complemented strain, *Moeri-1c* (Figure 13A-E, Figure 14). Conidial germination, appressorium formation, and pathogenicity of Δ*Moeri-1* were not changed like the Dicer-deleted mutants (Figure 15, Table 4).

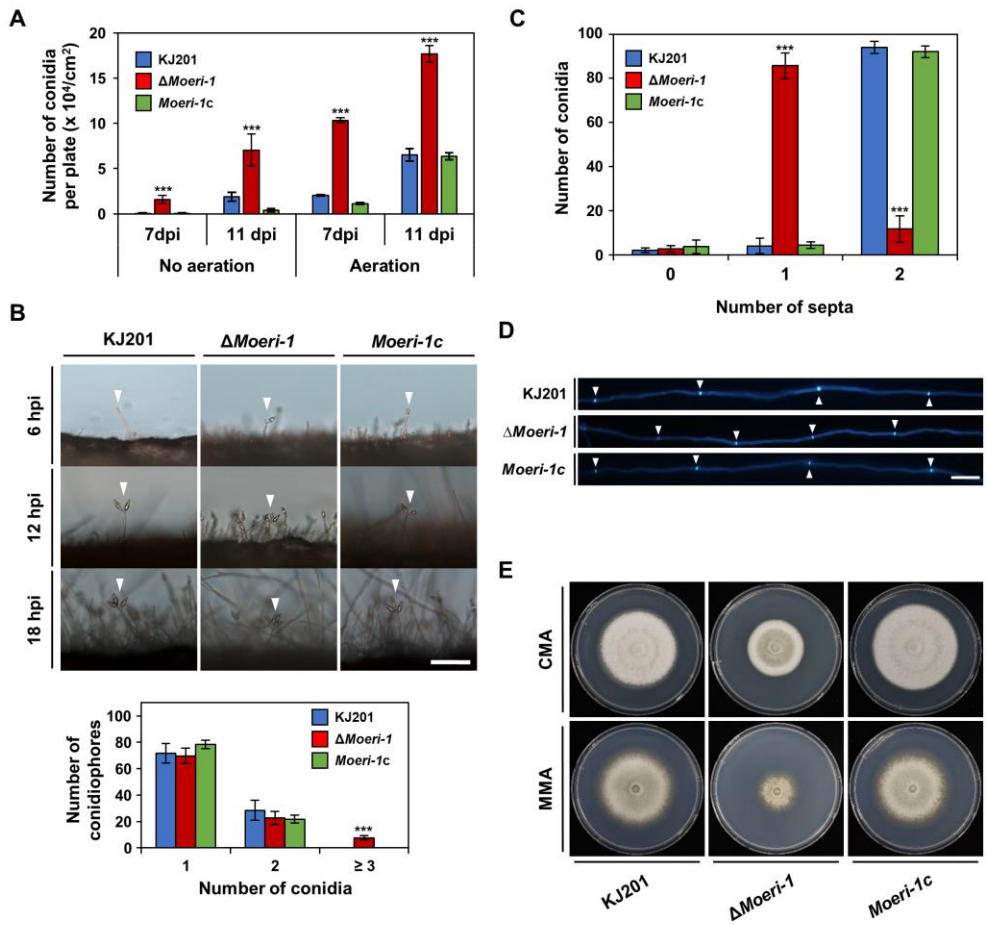


**Figure 13. Phenotypes of Δ*Moeri-1*. (A)** Conidiation assay of WT, Δ*Moeri-1*, and the *MoERI-1* complemented strain, *Moeri-1*c, with or without aeration. Conidia of each strain were collected at 7 and 11 days post-inoculation (dpi). Each strain was counted in triplicate. **(B)** Conidiophores were observed under light microscopy at 6, 12, and 18 hours post-induction (hpi). White arrowheads indicate the conidiophores with the conidia. One hundred conidiophores of each sample were counted at 12 hpi in triplicate. Scale bar, 40 μm. **(C)** The number of conidia according to septum number was counted. One hundred conidia of each sample were counted in triplicate. Error bars indicate the standard deviations of mean values. ***$p < 0.001$, Student's

*t*-test between the mean values of the WT and the mutant strains. **(D)** Calcofluor white staining of mycelial septa. Scale bar, 40 μm. **(E)** Mycelial growth on CMA and MMA at 25 °C 9 days post inoculation.

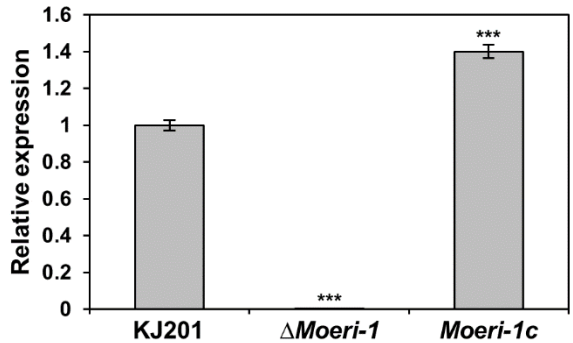


**Figure 14. Confirmation of gene deletion of MoERI-1 by qPCR.** Expression was measured in the WT, Δ*Moeri-1*, and the complemented strain *Moeri-1c* by qRT-PCR. β-tublin was used as a reference gene. Error bars indicate the standard deviations of mean values. ***$p < 0.001$, Student's t-test between the mean values of the WT and the mutant strains.

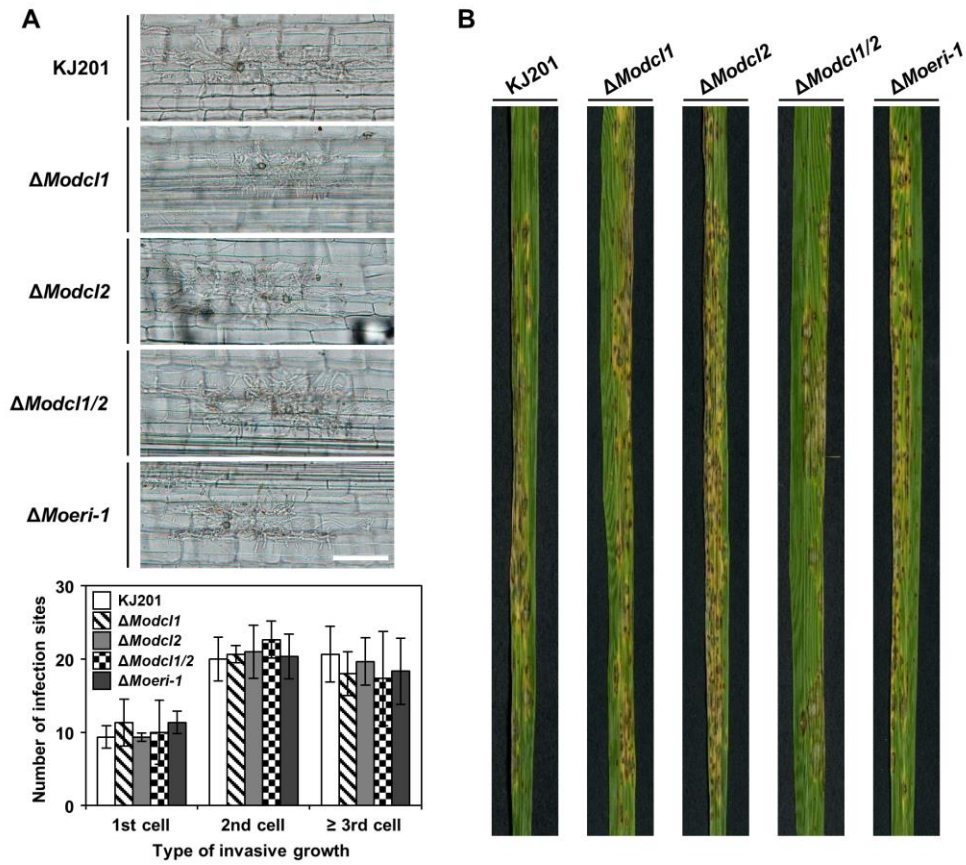


**Figure 15. Pathogenicity of *M oryzae* WT and deletion mutants. (A)** Conidial suspensions ($2 \times 10^4$/mL) were inoculated onto rice sheath cells of 6-week-old Nakdong. Invasive growth of the WT and deletion mutants in sheath cells at 48 hours post-inoculation was observed under light microscopy. The types of invasive growth were rated as 1st cell, 2nd cell, or ≥ 3rd cell colonization. Fifty infection sites of each sample were counted in triplicate. Error bars indicate the standard deviations of mean values. Student's *t*-test between the mean values of the WT and the mutant strains indicated that there are no significant differences. **(B)** 4-week-old cv. Nakdong rice seedlings were sprayed with conidial suspensions ($5 \times 10^4$/mL) of the WT and deletion mutant strains. Disease severity was measured at 7 days post-inoculation.

**Table 4. Conidial germination and appressorium formation of the strains**

| Strain | Germination* | Appressorium formation* |
|---|---|---|
| KJ201 | $92.3 \pm 0.6^{a,b**}$ | $98.6 \pm 1.5^{a}$ |
| Δ*Modcl1* | $93.7 \pm 0.6^{a}$ | $96.6 \pm 3^{a}$ |
| Δ*Modcl2* | $89.3 \pm 3.1^{b}$ | $98.6 \pm 1.2^{a}$ |
| Δ*Modcl1/2* | $94.3 \pm 1.5^{a}$ | $98.6 \pm 1.2^{a}$ |
| Δ*Moeri-1* | $91 \pm 2^{a,b}$ | $98.6 \pm 1.5^{a}$ |
| *Moeri-1*C | $94 \pm 3^{a}$ | $99.3 \pm 0.6^{a}$ |

*Values are means ± SD of three replications (n = 100).
**Values in the same column with the same superscript letter are not statistically different using Duncan's Multiple Range Test ($P < 0.05$).

## V. Transcriptome analysis of Δ*Moeri-1*

For further elucidation of the molecular mechanisms underlying altered phenotypes of Δ*Moeri-1,* we performed mRNA sequencing using total RNAs isolated from the mycelia and conidiation stage in the WT and in Δ*Moeri-1*. Deletion of *MoERI-1* altered the expression of 598 genes in mycelia and 811 genes in the conidiation stage. Gene Ontology (GO) enrichment analysis yielded 19 and 14 enriched GO terms in the DEGs of the mycelia and conidiation stages, respectively (Figure 16A). Among the down-regulated DEGs of the mycelia, 11 terms were enriched in biological processes (BP), 9 terms for "metabolic process" (e.g., "alpha-amino acid biosynthetic process"; GO: 1901607) and two for "transport" ("transmembrane transport"; GO: 0055085, and "phosphate ion transport"; GO: 0006817). One term, "inorganic phosphate transmembrane transporter activity" (GO: 0005315), was enriched in molecular function (MF). Among DEGs upregulated at the mycelia stage, no term was enriched in BP, two "protein binding"-related terms were enriched in MF ("protein dimerization activity"; GO: 0046983, and "protein heterodimerization activity"; GO: 0046982) and five terms related to "protein-containing complex" and "chromosome" (e.g. "nucleosome"; GO: 0000786, and "chromatin"; GO: 0000785) were enriched in cellular component (CC). Among downregulated DEGs at the conidiation stage, two "metabolic process" terms ("carbohydrate metabolic process"; GO: 0005975, and "oxidation-reduction process"; GO: 0055114), and one term, "transmembrane transport" (GO: 0055085) were enriched in BP. For the MF category, four "catalytic activity" terms, two "binding" and two "transporter activity" terms were enriched (e.g., "hydrolase

activity, hydrolyzing O-glycosyl compounds": GO: 0004553, "heme binding": GO: 0020037 and "transmembrane transporter activity"; GO: 0022857). Three terms enriched in CC were related to the term "membrane" (e.g., "integral component of membrane"; GO: 0016021).

We hypothesized that the direct or indirect effect of derepression of conidiation-related genes might affect the phenotypes of Δ*Moeri-1*. Therefore, we investigated overlaps between DEGs resulting from conidiation in the WT and *MoERI-1* mutants at the mycelia and conidiation stages. Of the genes upregulated by *MoERI-1* deletion at the mycelia stage, 48 % (160 of 334) overlapped with those up-regulated in the WT due to conidiation (Figure 16B). On the contrary, only 8 % (21 of 264) of the genes downregulated by the deletion of *MoERI-1* at the mycelial stage overlapped with those downregulated due to conidiation in the WT. Therefore, the up-regulated DEGs caused by deletion of *MoERI-1* in mycelia considerably overlapped with those up-regulated DEGs resulting from conidiation of the WT. Among the up-regulated DEGs were five genes (MAP kinase kinase kinase gene *MCK1*, mitophagy-related gene *MoATG24*, C2H2 zinc finger transcription factor *CONx6*, chitinase-coding gene *MoChia1,* and anti-apoptosis protein-coding gene *MoTCTP*), whose deletion mutants showed reduced conidiation (Jeon et al., 2008;He et al., 2013; Cao et al., 2016;Yang et al., 2019;Lilin et al., 2013). However, their expression was not significantly different at the conidiation stage between Δ*Moeri-1* and the WT. We also found genes encoding proteins important in cell cycle control such as *MoPCL1* and a homologue of kinetochore protein-encoding gene *MIS14* among the overlapped up-regulated genes (Lilin et al., 2013;Holt et al., 1996).

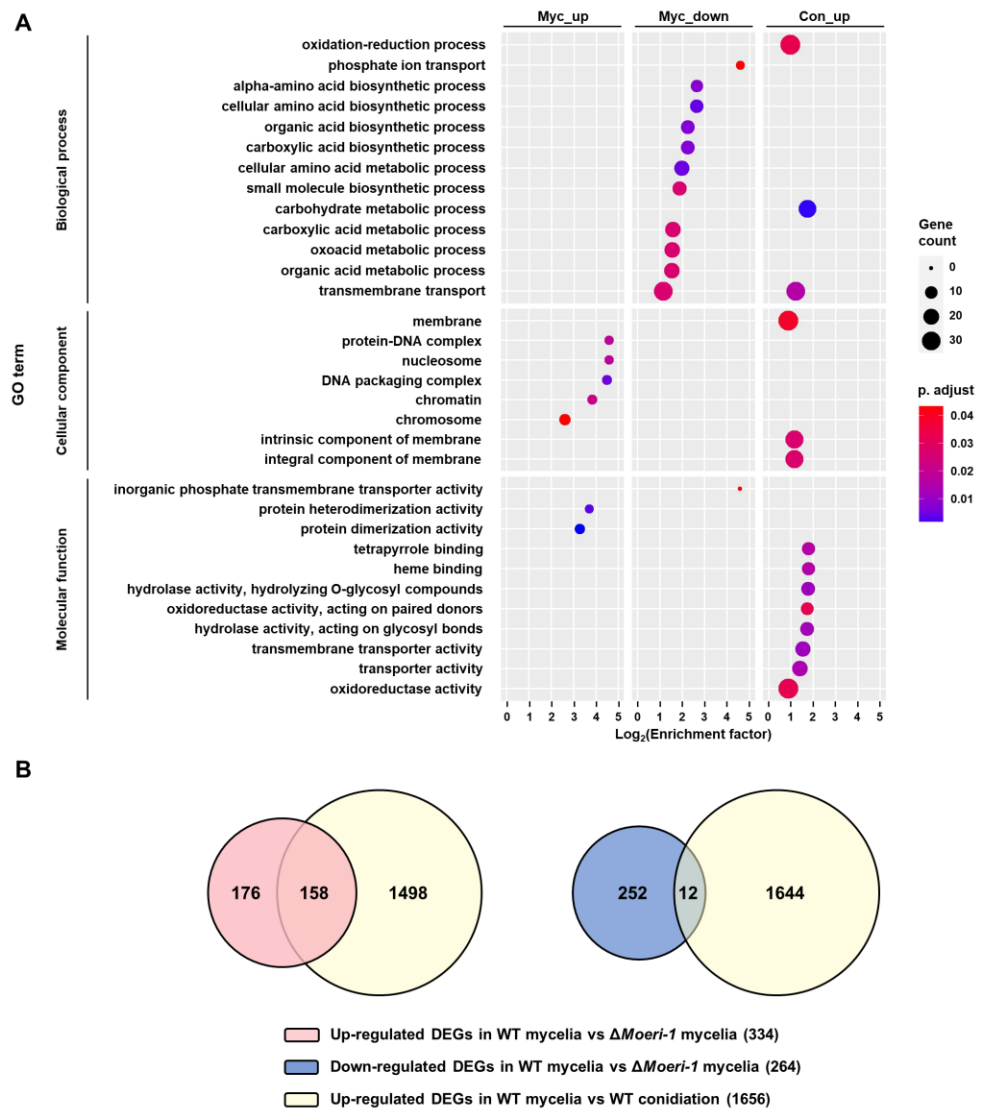


**Figure 16. DEG analyses between WT and Δ*Moeri-1*. (A)** GO enrichment analysis was performed for DEGs in mycelia of WT and Δ*Moeri-1*, and during conidiation in WT with BLAST2GO (Conesa and Götz, 2008). Circle size denotes the number of enriched genes; circle color denotes the adjusted p-value; *x*-axis, enrichment factor. **(B)** Venn diagram between the DEGs by *MoERI-1* deletion in mycelia and the up-DEGs during conidiation in WT.

## VI. Profiling of sRNAs in Δ*Moeri-1*

Based on the phylogenetic, phenotypic, and transcriptome data, we hypothesized that MoERI-1 regulates mRNA levels of other genes during the mycelia and conidiation stages. sRNA of the Δ*Moeri-1* from mycelia and conidiation stages were subjected to deep sequencing. Deletion of *MoERI-1* decreased the proportions of repeat-derived sRNAs (from 50% to 35%) and increased the read proportions of intergenic regions and structural RNAs (from 4% to 22% and 21% to 27%, respectively) at the conidiation stage (Figure 17). By contrast, 5'-end nucleotide proportions and length distributions were little affected by the deletion of *MoERI-1*. To investigate the relationship between Dicer proteins and MoERI-1, we compared MoERI-1-dependent sRNAs with Dicer-dependent or –independent sRNAs. 70% of the MoERI-1-dependent sRNAs were overlapped with Dicer-dependent sRNAs, and most of the overlapped total sRNAs were derived from repeat elements (81 %) (Figure 18A, B). These Dicer-dependent, MoERI-1-dependent sRNAs also shared the other features of Dicer-dependent sRNAs like 5' U preference and 23-nt length bias (Figure 18B, C). Meanwhile, Dicer-independent, MoERI-1-dependent sRNAs were mainly derived from tRNAs, and showed relatively irregular patterns in length distributions and nucleotide compositions (Figure 19B, C).

In a sRNA clustering analysis, 109 sRNA-producing loci showed a 4-fold decrease when *MoERI-1* was deleted. Among 109 MoERI-1-dependent sRNA loci, 50 loci were Dicer-independent but lacked specific sRNA features. Among the 109 loci, 22 were associated with repeat elements and 99 with 99 protein-coding genes (Table 3). Among the 99 protein-coding genes, the RNA seq data showed that six genes,

including *MoChia*, were upregulated in Δ*Moeri-1* (Figure 20).

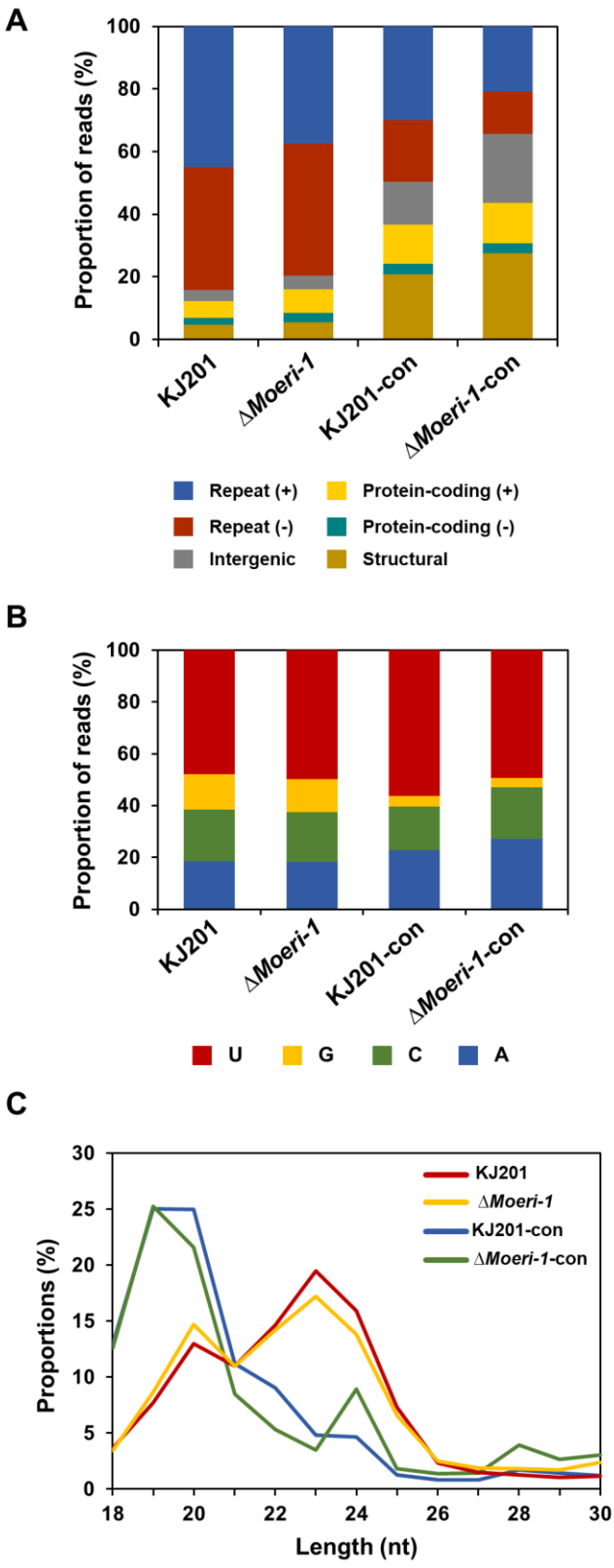
A
Proportion of reads (%)
100
80
60
40
20
0
KJ201
ΔMoeri-1
KJ201-con
ΔMoeri-1-con
Repeat (+)
Repeat (-)
Intergenic
Protein-coding (+)
Protein-coding (-)
Structural
B
Proportion of reads (%)
100
80
60
40
20
0
KJ201
ΔMoeri-1
KJ201-con
ΔMoeri-1-con
U
G
C
A
C
Proportions (%)
30
25
20
15
10
5
0
18
20
22
24
26
28
30
Length (nt)
KJ201
ΔMoeri-1
KJ201-con
ΔMoeri-1-con

**Figure 17. Profiling of sRNAs in the WT and Δ*Moeri-1* in the mycelia and during conidiation. (A)** Genomic origins of sRNAs. **(B)** 5'-end nucleotide preference. **(C)** Length distribution.

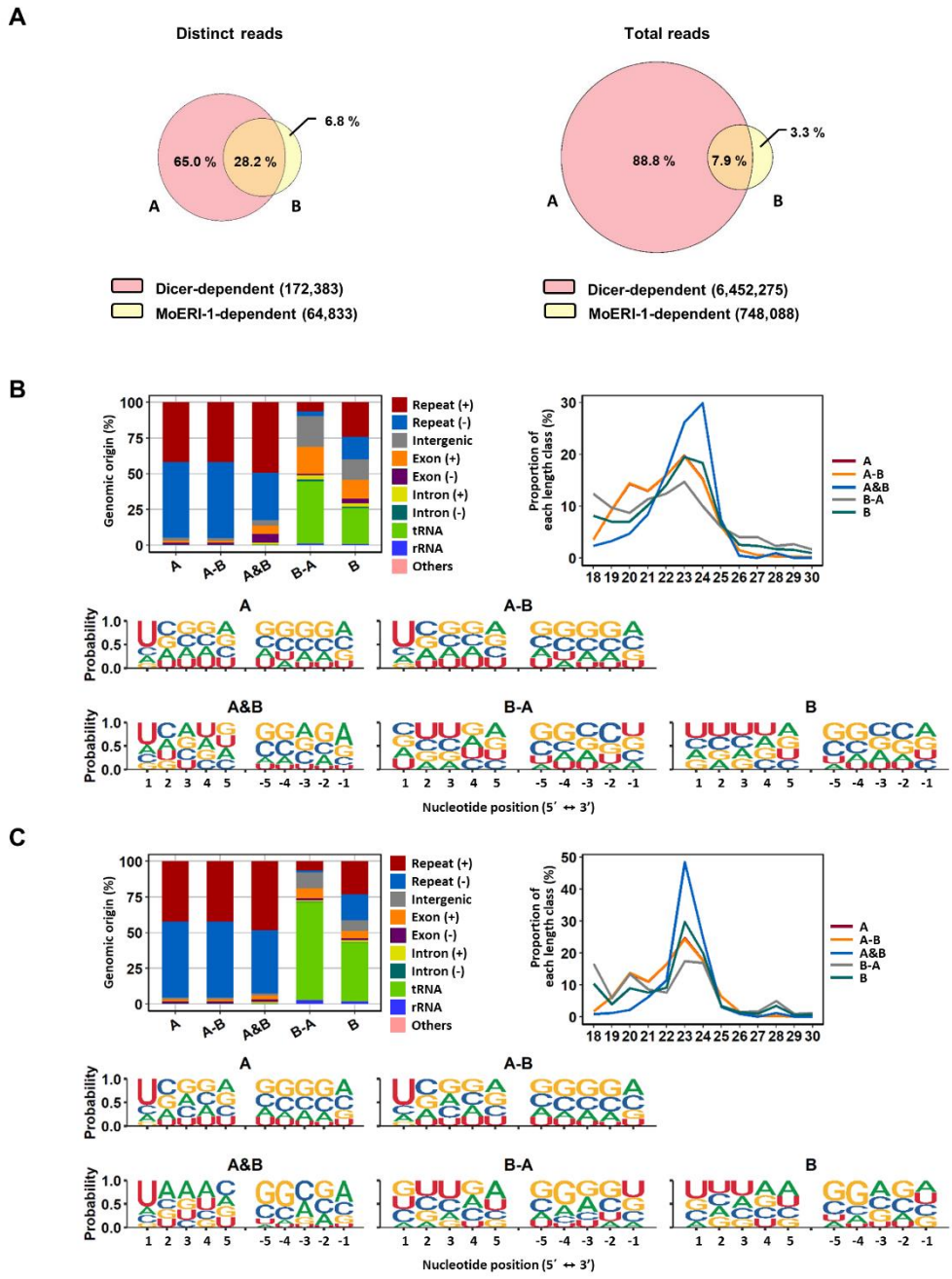


**Figure 18. Venn diagram of Dicer-dependent and MoERI-1-dependent reads using distinct and total sRNAs. (A)** Venn diagram of the proportions of distinct and total reads in the WT using Dicer-dependent and MoERI-1-

dependent reads. Genomic origin, length distribution, and nucleotide composition were investigated using the distinct **(B)** and total **(C).**

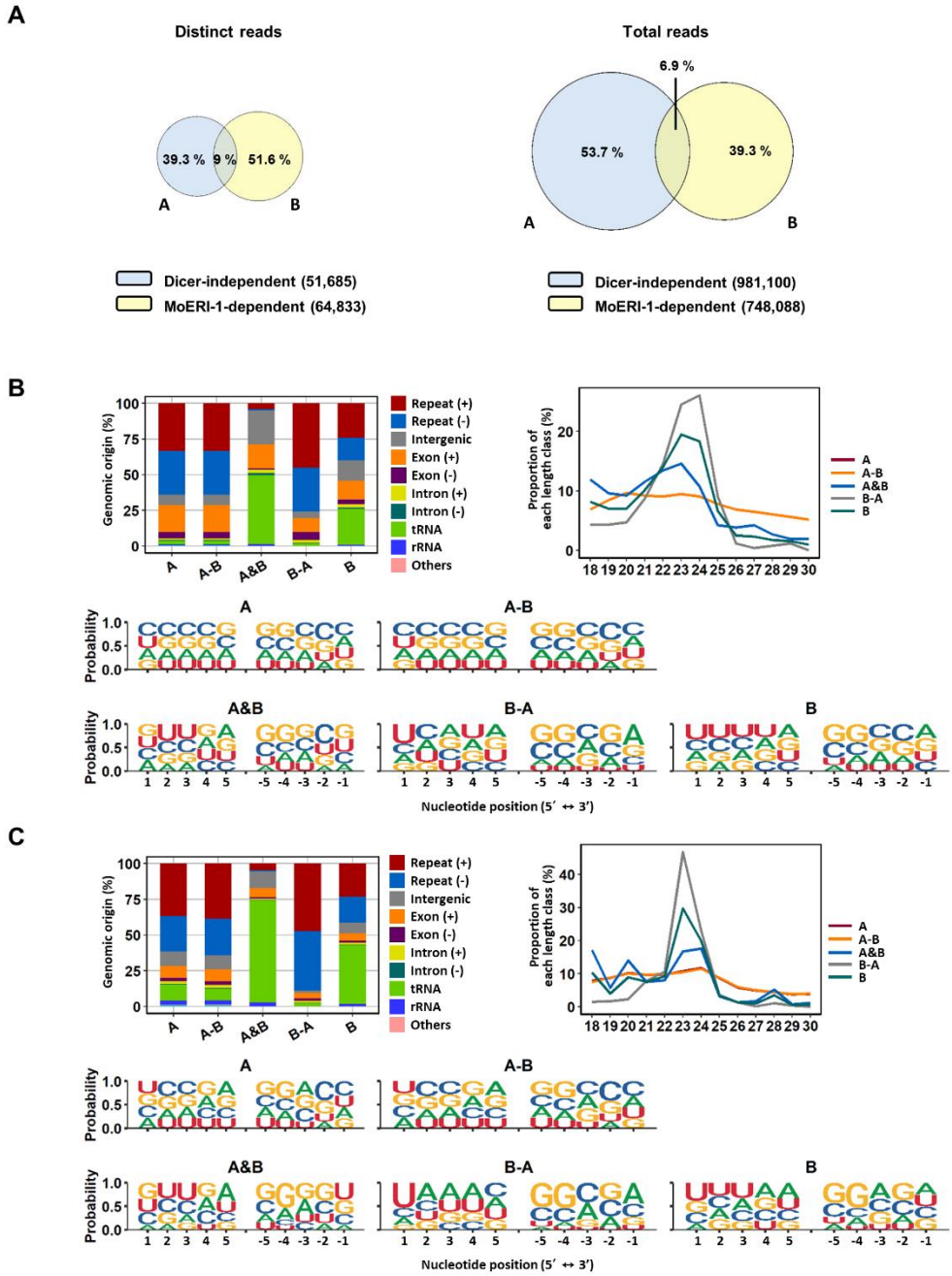


**Figure 19. Venn diagram of Dicer-independent reads and MoERI-1-dependent reads using distinct and total sRNAs. (A)** Venn diagram of the proportions of distinct and total reads in the WT using Dicer-independent and MoERI-1-dependent

reads. Genomic origin, length distribution, and nucleotide composition were investigated using the distinct **(B)** and total **(C)** reads**.**

# DISCUSSION

sRNAs generally have specific patterns such as length or nucleotide bias at a specific position, which were reported in both canonical and non-canonical RNAi (Mi et al., 2008;Lee et al., 2010;Nicolas et al., 2010). In this study, most *M. oryzae* sRNAs are 19–24-nt in length (Figure 4C). The deletion of *MoDCL2* led to disruption of the most length bias, while the deletion of *MoDCL1* caused a minor decrease of 23-24-nt sRNAs. Previously, sRNA sizes made by DCLs were experimentally speculated (Kadotani et al., 2008). The size distribution of siRNAs produced by *MoDCL1*-overexpressed mutant is included in the size distribution of siRNAs made by MoDCL2, but is concentrated within a relatively narrow range of longer sRNAs. However, with the normal level of expression, MoDCL1 was unable to make enough siRNAs to induce RNAi (Kadotani et al., 2008). Combined with our results, MoDCL2 is the major Dicer protein responsible for the biogenesis of 19-24-nt sRNAs, while MoDCL1 has a minor role in the production of 23-24-nt sRNAs during the mycelial stage.

Size distribution of *M. oryzae* sRNAs showed 23- and 20-nt as highest and second peaks, respectively (Figure 4C). It has been revealed that sRNAs of different lengths are involved in the discrete RNAi pathway in other eukaryotes (Hamilton et al., 2002). Two distinct classes of sRNAs (25–26- and 21-nt) have also been reported in an oomycete pathogen, *Phytophthora parasitica*, suggesting that the 25–26-nt class mediates RNAi. The 21-nt sRNAs, another major class, are involved with highly transcribed genomic loci in the WT (Jia et al., 2017). However, in *M. oryzae*, 20-nt

sRNA loci and 23-nt sRNA loci are highly correlated, indicating that most 20- and 23-nt sRNAs are derived from the same loci. Immature longer sRNAs undergo additional size processing after loading into AGO proteins in many organisms (Xue et al., 2012;Marasovic et al 2013). AGO proteins of *M. oryzae* bind to 20-nt siRNAs with uracil at the 5'-end, but do not participate in sRNA biogenesis (Nguyen et al., 2018;Raman et al., 2017). Considering the features of functional sRNAs, 23-nt sRNAs of *M. oryzae* may be processed into 20-nt class during the RNAi pathway.

We found that one of the WT libraries, KJL1 presented a distinct sRNA length distribution against other replicate libraries (KJL2 and KJL3) (Figure 2A, B). However, the sRNA-producing loci between replicates were highly correlated (Figure 2C). This result indicates that the sRNA loci repertoire was similar between replicates, but the length profiles of sRNAs derived from those loci were changed. In *M. oryzae*, diverse length distribution patterns have been reported not only according to various endogenous and environmental changes but also through the control WT libraries (Nguyen et al., 2018;Nunes et al., 2011;Raman et al., 2013;Raman et al., 2017). Combined with our results, these findings suggest that the length distribution of total sRNAs in *M. oryzae* is changed dynamically by apparent factors, including stress, tissue, and strain, and by unknown minor factors.

ex-siRNA (*F. graminearum* and *M. circinelloides*) and milRNA (*N. crassa* and *Penicillium marneffei*) are involved in the regulation of fungal gene expression (Nicolas et al., 2010;Lau et al., 2013;Lee et al., 2010). In *M. oryzae*, most Dicer-dependent sRNA loci within the genes were concentrated on the exon (Figure 6B; Figure 10A). sRNAs derived from the genes also showed lower strand-specificity

than those of Dicer-independent sRNAs, indicating *M. oryzae* sRNAs from genes were ex-siRNAs (Figure 10C). To find milRNA of *M. oryzae*, we performed miRNA loci prediction using software miREAP. However, we could not find miRNA loci with significant read numbers. A previous study found *milR236* by comparing sRNA libraries prepared from appressorium samples of *M. oryzae* strains. Overexpression of *milR236* caused suppression of *MoHat1*, leading to delayed appressorium formation (Li et al., 2020). We found that *milR236* was in the sRNA library of KJ201 WT, and its abundance was reduced in Δ*Modcl1/2* compared to the WT library. However, the sRNA-producing locus containing *milR236* was removed at the loci-filtering step because of the small read number. These findings imply that the lack of functional sRNAs in the KJ201 mycelial library might result from stage-specific expressions and roles of functional sRNAs, including *milR236*.

Deletion of *MoDCL* genes disrupted biased sRNA patterns. However, Dicer-independent sRNAs still had significant preferences on 20-nt with 5'U (Figure 4D). Moreover, Dicer-independent sRNAs showed cytosine bias at the penultimate position (Figure 10D). These specific patterns indicate a non-canonical, Dicer-independent RNAi pathway in *M. oryzae*. Similar to cytosine bias at the penultimate position in *M. oryzae*, rdrp-dependent degraded RNAs (rdRNAs) of *M. circinelloides* were reported to prefer uracil at the penultimate position (Trieu et al., 2015). RdRP and a non-canonical ribonuclease, R3B2 were necessary for the biogenesis and penultimate nucleotide bias of rdRNAs (Trieu et al., 2015). MoRdRP2 was reported to be involved in the canonical RNAi pathway, but the relevance between MoRdRP-dependent sRNA-producing loci and Dicer-independent sRNAs were not shown

(Raman et al., 2017). Additionally, we could not find the homologue of *R3B2* in *M. oryzae*. This implies that there should be an unknown Dicer-independent RNAi pathway exploiting penultimate-cytosine sRNAs. In *N. crassa*, sequencing of Ago-bound sRNA revealed a non-canonical sRNA, disiRNA with a 22-nt length bias and preference for uracil at the 5'-end (Lee et al., 2010). A homologue of *NcERI-1*, *MoERI-1* was identified, and associated sRNAs were profiled. Δ*Moeri-1* showed increased conidiation and reduced mycelial growth (Figure 13). Furthermore, comparison of mRNA and sRNA seq data revealed that MoERI-1-dependent sRNAs might be involved in gene regulation. However, unlike disiRNA of *N. crassa*, MoERI-1-dependent sRNAs showed an irregular pattern.

By comparative profiling, we found discrete features of sRNAs generated in Dicer-dependent and Dicer-independent manner. Based on the patterns of sRNAs in Δ*Modcl1/2*, we suggest the possibility of non-canonical RNAi pathways in *M. oryzae*. Furthermore, we identified a non-canonical RNAi component, *MoERI-1*, and revealed that MoERI-1 has roles in conidiation and septum formation of *M. oryzae*. Our study suggests the importance of non-canonical RNAi in the study of plant pathogenic fungi and may provide a novel roadmap for a comprehensive understanding of both canonical and non-canonical RNAi in fungi and beyond.

# LITERATURE CITED


Bai, Y., Lan, F., Yang, W., Zhang, F., Yang, K., Li, Z., et al. (2015). sRNA profiling in *Aspergillus flavus* reveals differentially expressed miRNA-like RNAs response to water activity and temperature. *Fungal Genet. Biol.* 81, 113-119.

Billmyre, R. B., Calo, S., Feretzaki, M., Wang, X., and Heitman, J. (2013). RNAi function, diversity, and loss in the fungal kingdom. *Chromosome Res.* 21, 561-572.

Buhler, M., and Moazed, D. (2007). Transcription and RNAi in heterochromatic gene silencing. *Nat. Struct. Mol. Biol.* 14, 1041-1048.

Calo, S., Nicolas, F. E., Lee, S. C., Vila, A., Cervantes, M., Torres-Martinez, S., et al. (2017). A non-canonical RNA degradation pathway suppresses RNAi-dependent epimutations in the human fungal pathogen *Mucor circinelloides*. *PLoS Genet.* 13, e1006686.

Cao, H., Huang, P., Zhang, L., Shi, Y., Sun, D., Yan, Y., et al. (2016). Characterization of 47 Cys2-His2 zinc finger proteins required for the development and pathogenicity of the rice blast fungus *Magnaporthe oryzae*. *New Phytol.* 211, 1035-1051.

Carreras-Villasenor, N., Esquivel-Naranjo, E. U., Villalobos-Escobedo, J. M., Abreu-Goodger, C., and Herrera-Estrella, A. (2013). The RNAi machinery regulates growth and development in the filamentous fungus *Trichoderma atroviride*. *Mol. Microbiol.* 89, 96-112.

Conesa, A., and Götz, S. (2008). Blast2GO: a comprehensive suite for functional

analysis in plant genomics. *Int. J. Plant Genomics 2008*.

Dang, Y., Cheng, J., Sun, X., Zhou, Z., and Liu, Y. (2016). Antisense transcription licenses nascent transcripts to mediate transcriptional gene silencing. *Genes Dev.* 30, 2417-2432.

Dean, R., Van Kan, J. A. L., Pretorius, Z. A., Hammond-Kosack, K. E., Di Pietro, A., Spanu, P. D., et al. (2012). The Top 10 fungal pathogens in molecular plant pathology. *Mol. Plant Pathol.* 13, 414-430.

Dong, S., Raffaele, S., and Kamoun, S. (2015). The two-speed genomes of filamentous pathogens: waltz with plants. *Curr. Opin. Genet.* 35, 57-65

Drinnenberg, I. A., Weinberg, D. E., Xie, K. T., Mower, J. P., Wolfe, K. H., Fink, G. R., et al. (2009). RNAi in Budding Yeast. *Science* 326, 544-550.

Ghildiyal, M., and Zamore, P. D. (2009). Small silencing RNAs: an expanding universe. *Nat. Rev. Genet.* 10, 94-108.

Goh, J., Kim, K. S., Park, J., Jeon, J., Park, S. Y., and Lee, Y. H. (2011). The cell cycle gene MoCDC15 regulates hyphal growth, asexual development and plant infection in the rice blast pathogen *Magnaporthe oryzae*. *Fungal Genet. Biol.* 48, 784-792.

He, Y., Deng, Y. Z., and Naqvi, N. I. (2013). Atg24-assisted mitophagy in the foot cells is necessary for proper asexual differentiation in *Magnaporthe oryzae*. *Autophagy* 9, 1818-1827.

Holt, C. L., and May, G. S. (1996). An extragenic suppressor of the mitosis-defective *bimD6* mutation of *Aspergillus nidulans* codes for a chromosome scaffold protein. *Genetics* 142, 777-787.

Jeon, J., Goh, J., Yoo, S., Chi, M. H., Choi, J., Rho, H. S., et al. (2008). A putative

MAP kinase kinase kinase, *MCK1*, is required for cell wall integrity and pathogenicity of the rice blast fungus, *Magnaporthe oryzae*. *Mol. Plant Microbe Interact.* 21, 525-534.

Johnson, N. R., Yeoh, J. M., Coruh, C., and Axtell, M. J. (2016). Improved placement of multi-mapping small RNAs. *G3 (Bethesda)* 6, 2103-2111.

Joshi, N.A., and Fass, J.N. (2011). Sickle: a sliding-window, adaptive, quality-based trimming tool for FastQ files. Version 1.33. https://github.com/najoshi/sickle.

Kadotani, N., Nakayashiki, H., Tosa, Y., and Mayama, S. (2004). One of the two Dicer-like proteins in the filamentous fungi *Magnaporthe oryzae* genome is responsible for hairpin RNA-triggered RNA silencing and related small interfering RNA accumulation. *J. Biol. Chem.* 279, 44467-44474.

Kadotani, N., Murata, T., Quoc, N. B., Adachi, Y., and Nakayashiki, H. (2008). Transcriptional control and protein specialization have roles in the functional diversification of two Dicer-like proteins in *Magnaporthe oryzae*. *Genetics* 180, 1245-1249.

Kim, D., Paggi, J. M., Park, C., Bennett, C., and Salzberg, S. L. (2019). Graph-based genome alignment and genotyping with HISAT2 and HISAT-genotype. *Nat. Biotechnol*. 37, 1.

Kim, S., Ahn, I. P., Rho, H. S., and Lee, Y. H. (2005). MHP1, a *Magnaporthe grisea* hydrophobin gene, is required for fungal development and plant colonization. *Mol. Microbiol.* 57, 1224-1237.

Langmead, B., Trapnell, C., Pop, M., and Salzberg, S.L. (2009). Ultrafast and memory-efficient alignment of short DNA sequences to the human genome.

*Genome Biol*. 10, R25.

Lau, G. W., and Hamer, J. E. (1998). Acropetal: a genetic locus required for conidiophore architecture and pathogenicity in the rice blast fungus. *Fungal Genet. Biol.* 24, 228-239.

Lee, H. C., Li, L., Gu, W., Xue, Z., Crosthwaite, S. K., Pertsemlidis, A., et al. (2010). Diverse pathways generate microRNA-like RNAs and Dicer-independent small interfering RNAs in fungi. *Mol. Cell* 38, 803-814.

Lee, J., Lee, T., Lee, Y. W., Yun, S. H., and Turgeon, B. G. (2003). Shifting fungal reproductive mode by manipulation of mating type genes: obligatory heterothallism of *Gibberella zeae*. *Mol. Microbiol.* 50, 145-152.

Lilin, Z., Huijuan, C., Xiaodong, L., Fucheng, L., Xiaoxiao, F., and Jianping, L. (2013). *MoTCTP*, a homolog of translationally controlled tumor protein, is required for fungal growth and conidiation in *Magnaporthe oryzae*. *Chinese. J. Cell. Biol*. 35, 1141-1154.

Lim, Y.-J., Kim, K. T., and Lee, Y. H. (2018). SUMOylation is required for fungal development and pathogenicity in the rice blast fungus *Magnaporthe oryzae*. *Mol. Plant Pathol*. 19, 2134-2148.

Lim, Y.-J., and Lee, Y.-H. (2020). F-box only and CUE proteins are crucial ubiquitination-associated components for conidiation and pathogenicity in the rice blast fungus, *Magnaporthe oryzae*. *Fungal Genet. Biol.* 144, 103473.

Marasovic, M., Zocco, M., and Halic, M. (2013). Argonaute and Triman generate Dicer-independent priRNAs and mature siRNAs to initiate heterochromatin formation. *Mol. Cell* 52, 173-183.

Martin, M. (2011). Cutadapt removes adapter sequences from high-throughput

sequencing reads. *EMBnet.journal* 17,10–12.

Nguyen, Q., Iritani, A., Ohkita, S., Vu, B. V., Yokoya, K., Matsubara, A., et al. (2018). A fungal argonaute interferes with RNA interference. *Nucleic Acids Res.* 46, 2495-2508.

Nicolas, F. E., Moxon, S., de Haro, J. P., Calo, S., Grigoriev, I. V., Torres-Martinez, S., et al. (2010). Endogenous short RNAs generated by Dicer 2 and RNA-dependent RNA polymerase 1 regulate mRNAs in the basal fungus *Mucor circinelloides*. *Nucleic Acids Res.* 38, 5535-5541.

Nicolás, F. E., and Ruiz-Vázquez, R. M. (2013). Functional diversity of RNAi-associated sRNAs in fungi. *International journal of molecular sciences* 14, 15348-15360.

Nunes, C. C., Gowda, M., Sailsbery, J., Xue, M., Chen, F., Brown, D. E., et al. (2011). Diverse and tissue-enriched small RNAs in the plant pathogenic fungus, *Magnaporthe oryzae*. *BMC Genomics* 12, 1-20.

Park, S.-Y., Choi, J., Lim, S.-E., Lee, G.-W., Park, J., Kim, Y., et al. (2013). Global expression profiling of transcription factor genes provides new insights into pathogenicity and stress responses in the rice blast fungus. *PLoS Path.* 9, e1003350.

Patel, R. K., and Jain, M. (2012). NGS QC Toolkit: a toolkit for quality control of next generation sequencing data. *PloS one* 7, e30619.

Pertea, M., Pertea, G. M., Antonescu, C. M., Chang, T. C., Mendell, J. T., and Salzberg, S. L. (2015). StringTie enables improved reconstruction of a transcriptome from RNA-seq reads. *Nat. Biotechnol.* 33, 290-295.

Raman, V., Simon, S. A., Romag, A., Demirci, F., Mathioni, S. M., Zhai, J., et al.

(2013). Physiological stressors and invasive plant infections alter the small RNA transcriptome of the rice blast fungus, *Magnaporthe oryzae*. *BMC Genomics* 14, 1-18.

Raman, V., Simon, S. A., Demirci, F., Nakano, M., Meyers, B. C., and Donofrio, N. M. (2017). Small RNA functions are required for growth and development of *Magnaporthe oryzae*. *Mol. Plant Microbe Interact.* 30, 517-530.

Siomi, M. C., Sato, K., Pezic, D., and Aravin, A. A. (2011). PIWI-interacting small RNAs: the vanguard of genome defence. *Nat. Rev. Mol. Cell Biol.* 12, 246-258.

Son, H., Park, A. R., Lim, J. Y., Shin, C., and Lee, Y. W. (2017). Genome-wide exonic small interference RNA-mediated gene silencing regulates sexual reproduction in the homothallic fungus *Fusarium graminearum*. *PLoS Genet.* 13, e1006595.

Thomas, M. F., L'Etoile, N. D., and Ansel, K. M. (2014). Eri1: a conserved enzyme at the crossroads of multiple RNA-processing pathways. *Trends Genet.* 30, 298-307.

Torres-Martinez, S., and Ruiz-Vazquez, R. M. (2017). The RNAi universe in fungi: a varied landscape of small RNAs and biological functions. *Annu. Rev. Microbiol.* 71, 371-391.

Wang, B., Sun, Y., Song, N., Zhao, M., Liu, R., Feng, H., et al. (2017). *Puccinia striiformis* f. sp. *tritici* mi croRNA-like RNA 1 (*Pst-milR1*), an important pathogenicity factor of *Pst*, impairs wheat resistance to *Pst* by suppressing the wheat pathogenesis-related 2 gene. *New Phytol.* 215, 338-350.

Weiberg, A., Wang, M., Lin, F.-M., Zhao, H., Zhang, Z., Kaloshian, I., et al. (2013).

Fungal small RNAs suppress plant immunity by hijacking host RNA interference pathways. *Science* 342, 118-123.

Yang, C., Yu, Y., Huang, J., Meng, F., Pang, J., Zhao, Q., et al. (2019). Binding of the *Magnaporthe oryzae* chitinase MoChia1 by a rice tetratricopeptide repeat protein allows free chitin to trigger immune responses. *Plant Cell* 31, 172-188.

Ye, R., Chen, Z., Lian, B., Rowley, M. J., Xia, N., Chai, J., et al. (2016). A Dicer-Independent Route for Biogenesis of siRNAs that Direct DNA Methylation in *Arabidopsis*. *Mol. Cell* 61, 222-235.

# 유전체 수준의 벼도열병균 소형 RNA 분석

이 현 준

## 초 록

RNA 간섭(RNAi)은 소형 RNA(sRNA)에 의해 매개되는 유전자 발현을 억제하는 잘 보존된 메커니즘이다. 소형 RNA는 서열 상보적인 방법을 사용하여 RNA에 의해 유도되는 유전자 침묵 복합체(RISC)를 표적 mRNA로 유도하며, 이를 통해 메신저 RNA(mRNA)의 분해, 번역 억제 또는 전사 억제를 통해 유전자를 조절한다. RNA 간섭 구성 요소의 기능적 특성화에 대한 최근의 연구는 RNA 간섭이 기주 식물에 대한 진균의 병 발생에 필수적인 역할을 한다는 것을 보여주었다. RNA 간섭에 의해 조절되는 곰팡이 표적 바이러스의 방어 및 스트레스 내성 또한 일부 식물 병원균이 완전한 병원성을 유지하는 데 중요하다. 최근들어 여러 식물 병원성 곰팡이에서 유래하는 소형 RNA가 숙주 식물로 분비되고 숙주 유전자 발현을 조절할 수 있다는 것이 밝혀졌다. 이러한 연구결과들은 식물 병원성 곰팡이가 다양한 과정에서 RNAi 메커니즘을 이용하여 병원성을 조절한다는 것을 시사한다. 또한, 핵심 RNAi 성분인 다이서(Dicer) 또는 아고넛(Argonaute) 단백질이 관여하지 않는 비표준

RNAi 경로는 동물, 식물 및 곰팡이에서 중요한 역할을 하는 것으로 보고된 바 있다. 그러나 식물 병원균과 비표준적 RNA 간섭의 관련성은 거의 연구되지 않았다. 본 연구에서는 도열병의 원인균인 *Magnaporthe oryzae*에서 비표준적이고 다이서 독립적인 RNA 간섭에 대한 포괄적인 이해를 위해, 다이서 의존적인 소형 RNA와 다이서 독립적인 소형 RNA를 비교 분석했다. 다이서 의존적 소형 RNA는 길이가 19-24-nt이고 가닥 특이성이 낮았다. 대조적으로, 다이서 독립적인 소형 RNA는 높은 가닥 특이성과 불규칙한 길이 패턴을 나타냈다. 다이서 의존적 소형 RNA가 5' 말단에서 유라실(uracil) 에 대한 선호도를 보인 반면, 다이서 독립적 sRNA는 3’ 말단으로부터 두번째 염기가 사이토신(cytosine)으로 편향되었다. 다이서 의존적 소형 RNA가 유래하는 게놈(genome) 지역은 주로 LTR(Long terminal repeat)-전이인자와 관련이 있는 반면, 다이서 독립적 sRNA는 단백질 코딩 유전자와 주로 연관된 것으로 나타났다. 벼도열병균의 다이서 독립적인 sRNA의 역할을 연구하기 위해, 본 연구에서는 비표준 RNAi 구성 요소이자 *Neurospora crassa ERI-1* 유전자의 상동체인 *MoERI-1*를 찾아냈다. *MoERI-1*의 삭제 돌연변이체가 무성생식 포자 생산이 증가하는 표현형을 나타냈기에, 균사체와 무성생식 포자 생산 단계에서 *MoERI-1* 삭제 돌연변이체의 RNA를 분리하여 소형 RNA와 메신저 RNA 염기 서열 분석을 수행하였다. 염기서열 분석 결과를 통해 *MoERI-1*의 삭제는 무성 생식 포자 생산과 세포 주기에 관여하는 유전자의 발현을 증가시킴을 확인할 수 있었다.

또한, 소형 RNA와 메신저 RNA 전사체의 비교를 통해, MoERI-1 의존적 소형 RNA가 유전자 발현 조절을 매개한다는 것이 밝혀졌다. 종합하여, 벼도열병균은 Dicer 독립적인 비표준 RNA간섭 경로를 가지며, 무성생식포자 생산 과정을 조절하기 위해 MoERI-1 의존적 소형 RNA를 이용함을 밝혔다.

**주요어 :** 벼도열병균, 소형 RNA, RNA 간섭, Dicer 비의존성, MoERI-1
**학번** : 2014-22938